

# Chemical, multi-isotopic (Li-B-Sr-U-H-O) and thermal characterization of Triassic formation waters from the Paris Basin

R. Millot<sup>1\*</sup>, C. Guerrot<sup>1</sup>, C. Innocent<sup>1</sup>, Ph. Négrel<sup>1</sup> and B. Sanjuan<sup>2</sup>

(1) BRGM, Metrology Monitoring Analysis Department, Orléans, France

(2) BRGM, Department of Geothermal Energy, Orléans, France

\* Corresponding author, e-mail: r.millot@brgm.fr

---

## Abstract

This work reports chemical and isotope data and temperature estimates for seven water samples collected from Triassic formations in the Paris Basin in France. Four samples were collected in the central part of the Basin (saline waters) and three were collected at the edge of the Basin near the recharge zone (dilute waters). The saline waters collected from the Chaunoy and Champotran boreholes have high salinities (around 120 g/L) and very similar chemical and isotopic compositions. The saline water sample from the La Torche borehole has much higher salinity (168 g/L) and significantly different isotope characteristics. The chemical geothermometers applied to these fluids from the centre of the Basin give temperature values ranging between 80 and 100°C. The fresh water samples collected at the edge of the Basin have very different chemical and isotopic compositions. These dilute water samples (Santenay and Châteauroux) are shallow, with colder temperatures of around 45 to 50°C. The study of uranium activity ratios for these Triassic formation waters allows us, as a first approximation, to estimate a mean apparent fluid circulation velocity of around 0.2 m/yr, which corresponds to a "mean age" slightly higher than 1 My for waters sampled in the Chaunoy, Champotran and La Torche fields in the centre of the Basin. The multi-isotope characterization of Triassic formation waters shows that our data are in agreement with literature values as concerns "traditional" isotope systematics ( $\delta^{18}\text{O}$ ,  $\delta\text{D}$ ,  $^{87}\text{Sr}/^{86}\text{Sr}$ ). Li and B isotope signatures in the centre of the Paris basin are in a good agreement with a fluid signature derived mainly from water/rock interactions involving clastic rocks with water essentially resulting from a seawater-derived brine endmember diluted by meteoric waters. The data reported in the present work for Li and B isotopes could be used as a reference for future studies to characterize sandstone formation waters.

**Keywords:** lithium isotopes, boron isotopes, strontium isotopes, uranium isotopes, oxygen isotopes, hydrogen isotopes, geothermometry, Trias, Paris Basin

## 1. INTRODUCTION

The Paris Basin is an intracratonic basin, covering approximately 6,000 km<sup>2</sup>, filled with up to 3,000 m of sediments overlying the Hercynian basement (Pomerol 1974). Sediments range in age from Permian to Quaternary. There are six major aquifer formations in the Paris Basin, ranging in age from Trias to Cenozoic, of which the deepest are the Triassic sandstones and the Dogger limestones. Both include oil accumulations associated with occurrences of saline groundwaters, and there are small oil fields East of Paris. Low enthalpy geothermal fluids are another economic benefit associated with these deep aquifers since water temperatures in the deepest part of these aquifers may be relatively high (around 100°C).

Within the framework of the development of renewable energy in France, a research project involving an inventory of geothermal resources has been carried out jointly by the French Agency for Environment and Energy Management (ADEME) and the French Geological Survey (BRGM). The CLASTIQ research project (CLAyed sandSTone In Question) focuses on the sandstone geothermal reservoirs in France (Bouchot et al. 2008).

The present study deals with the geochemistry of both saline and dilute waters from the Triassic aquifer sampled in the Paris Basin. Several studies were carried out in the 1990's to reconstruct the history of the deep waters of the Paris Basin. Based on the combination of major elements and water stable isotopes ( $\delta D$  and  $\delta^{18}O$ ), it was shown that the western Keuper brines could derive from the dissolution of eastern Triassic salts by the input of meteoric water and that the Dogger formation waters could originate mainly from Triassic inputs via faults. In greater detail, Fontes and Matray (1993a) reported chemical data for brines associated with the Triassic saline deposits in the Paris Basin. This study showed that the brines collected in the eastern part of the Paris Basin were made up of a mixture of both primary and secondary brines, and that Permian evaporites might contribute to the chemical signature of the Triassic formation waters under consideration. These authors also studied waters from the oil-bearing Triassic formations (Keuper and Rhaetian) (Fontes and Matray, 1993b) and confirmed that the saline waters from Dogger, Keuper and Rhaetian formations have a complex origin and might come from various mixtures. The salinity of the Dogger and Keuper waters originates from brine having a primary origin. Rhaetian waters have salinities that can be explained by the contribution of three different origins: (i) a primary brine identical to that of the Dogger and Keuper, (ii) seawater and (iii) a dilution by meteoric water.

Matray et al. (1994) investigated Dogger formation waters in the Paris Basin and suggested a possible exchange of groundwaters in the Dogger and Triassic aquifers by the migration of brine from the Triassic to the Dogger formation. Other exchanges between Jurassic and Triassic aquifers are discussed by Worden et al. (1999), in particular for the "Chaunoy Sandstones Formation". These authors suggested that waters from the Triassic Chaunoy

formation might migrate towards the Dogger formation to compensate for the meteoric contribution. Matray et al. (1989) also discussed the diagenetic effects on the Dogger and Triassic reservoirs of the Paris Basin and proposed a scenario of evolution. The results of their analyses of water from the Dogger and Triassic formations show that each reservoir has a specific mixture of (i) a hot, saline endmember made up of primary and secondary brines having a Triassic origin, and (ii) a weakly concentrated endmember of meteoric origin that dilutes the waters. The different mixtures are the result of considerable circulation of solutions between the reservoirs, thus suggesting the widespread migration of solutes with time. The results of Matray et al. (1989) also make it possible to reconstitute a complex diagenetic history based on the chronology of the water/rock interactions.

In this paper, we report chemical and isotope data from Triassic formation waters collected in the Paris Basin in order to provide further constraints on the characterization of the Triassic reservoir. The present study aims therefore to answer remaining questions about Triassic formation waters : what is the origin of the salinity of the brines from the Paris Basin, is there any exchange between the Triassic aquifer and the Dogger aquifer, what is the fluid circulation velocity of waters between the recharge zone and the centre of the basin. More specifically, the main objective of the present work is to constrain the nature and temperature of these fluids: two essential parameters for the characterization of a geothermal reservoir.

The data reported here for Triassic formation waters are the major and trace elements and a broad range of isotope data: “traditional” isotope systematics like the stable oxygen and hydrogen isotopes of the water molecule and Sr and U isotopes, and “non traditional” isotope systematics like Li and B isotopes.

Major and trace elements are first investigated in order to determine the chemical signature of the Triassic formation waters. A multi-isotopic approach is then used to provide additional information for the characterization of these waters. The stable isotopes of the water molecule ( $\delta D$  and  $\delta^{18}O$ ) are studied in order to define the origin of the waters. Sr isotopes ( $^{87}Sr/^{86}Sr$ ) are also investigated in order to better define the signature of the reservoir the waters come from. The isotopic composition of boron ( $\delta^{11}B$ ) is determined in an attempt to elucidate the source of B. The use of Li isotopic systematics ( $\delta^7Li$ ) is also explored, following recent papers indicating that Li isotopes seem to be an effective tracer of water/rock interactions in groundwaters (Millot et al. 2007, Millot and Négrel 2007). Uranium isotopes are also investigated in order to constrain the time of water transfer through the sedimentary basin. Lastly, a thermal characterization of these Triassic formations waters is proposed in order to enable the evaluation of potential geothermal resources.

## 2. SAMPLES

The different fluids (n=7) analysed in the present study were sampled between November 2007 and May 2008 in 3 locations: (1) in the Chaunoy, Champotran and La Torche oil fields, (2) near the city of Châteauroux, and (3) near the town of Santenay. Groundwater samples were drawn from the Triassic aquifer in the centre of the Paris Basin (Chaunoy, Champotran and La Torche, n=4) and near the recharge zone at the edge of the Basin (Châteauroux and Santenay, n=3) (Figure 1).

In total, only four samples were collected in the central part of the Basin (saline waters) and three were collected at the edge of the Basin near the recharge zone (dilute waters). Here, we would like to highlight the fact that the sampling of these deep waters is very difficult and that there are only few boreholes allowing the sampling of such deep waters within the Paris Basin.

### 2.1. Chaunoy, Champotran and La Torche

Triassic fluids were sampled from the Chaunoy, Champotran and La Torche oil fields in November 2007. The characteristics of the four boreholes are given in Table 1. The Chaunoy, Champotran and La Torche boreholes are between 2,449 and 2,989 m deep and the water content of the fluids varies between 15.6 and 97%. An anhydritic clay layer (Upper Keuper) of the Chaunoy Sandstones Formation is sampled by the Chaunoy72, Chaunoy73 and CHAN25 boreholes, and a green clay layer by the LT09 borehole.

The fluids from the Chaunoy, Champotran and La Torche oil fields contain hydrocarbons in various proportions. In order to separate the various phases from the fluid, we separated the water from the water-hydrocarbon mixture either in the field during sampling for Chaunoy72 or, for the other samples, a few days later in the laboratory. The device used in the field makes it possible to separate the 3 phases (oil-gas-water) from the fluid directly after collection at the top of the well. Once collected, the 3-phase fluid flows into a ~120 L polypropylene cylinder. Emulsion takes place in this part of the device. The excess gas escapes through the top of the device and water is sampled at the bottom. Since there can still be traces of hydrocarbon remaining the water at this stage of the separation, another cylinder containing rockwool filters the water before its physicochemical parameters are measured. The water is then collected at the outlet of the device and filtrated at 0.2 µm.

For the other samples, the water was separated in the laboratory after the mixture was collected in the field (water + hydrocarbons). Samples were put in a drying oven at a temperature of 50°C in 5-liter containers having a broad surface of contact. After 48 h, the

recovery rates of water were satisfactory and we were able to collect sufficient volumes of water for the chemical and isotopic analyses.

Possible contamination using both devices was tested by the determination of a blank using pure water solution (Milli-Q® water) after evaporation and filtration. This test clearly showed that there is no contamination for major or trace elements from containers or during handling either in the field or in the laboratory.

## **2.2. Châteauroux**

GTH1 was sampled near Châteauroux (ZAC St Jean). References for this borehole are GTH1: 05447X0112. The temperature at the wellhead of this 670-meter-deep well is 34°C. GTH1 taps the sandy Keuper aquifer formation of the Donnemarie Sandstones Formation.

## **2.3. Santenay**

The Santenay boreholes are located in a Triassic sandy sedimentary area overlying the Hercynian basement of the Morvan Massif with bedrock outcroppings located nearby, to the West. The two natural thermal springs – Lithium (due to the high Li content of this thermal spring) and Santana – were tapped by drilling (to depths of 75 and 88 m, respectively). We do not know the name of the sandy reservoir that was sampled here. The Lithium spring (code 05531X0018; geographical coordinates NGF: X = 779.040 km, Y = 2 216.620 km; Z = 225 m) and the Santana spring were sampled in May 2008.

## **3. METHODS**

All the chemical analyses were done in the BRGM laboratories using standard water analysis techniques such as ion chromatography, atomic absorption spectrophotometry, inductively coupled plasma mass spectrometry (ICP-MS), colorimetry, ion electrode and titration. The accuracy of the major and trace element data is about  $\pm 5\%$ . Major species and trace elements were determined on conditioned samples, i.e. after filtration at 0.2  $\mu\text{m}$  for the major anions, and after filtration at 0.2  $\mu\text{m}$  and acidification with Suprapur  $\text{HNO}_3$  acid (down to pH = 2) for the major cations and trace elements.

Accuracy and precision for major and trace elements was verified by repeated measurements of standard materials during the course of this study: namely Ion96-3 and LGC6020 for cations and anions and pure Li and B standard solutions (Merck) for Li and B determinations. For saline samples, they were analysed either after dilution (to minimize

matrix effects during measurement) or by using the technique of the standard addition (to match the matrixes of the standard materials).

### 3.1. Hydrogen and oxygen isotopes

Oxygen and hydrogen isotope measurements were done in BRGM's stable isotope laboratory with a standardized method, using a Finnigan MAT 252 mass spectrometer with a precision of  $\pm 0.1\text{‰}$  vs. SMOW for  $\delta^{18}\text{O}$  and  $\pm 0.8\text{‰}$  for  $\delta\text{D}$  respectively. Isotopic compositions are reported in the usual  $\delta$ -scale in ‰ according to  $\delta_{\text{sample}} (\text{‰}) = \{(R_{\text{sample}}/R_{\text{standard}}) - 1\} \times 1000$ , where R is the  $^2\text{H}/^1\text{H}$  or  $^{18}\text{O}/^{16}\text{O}$  atomic ratios.

### 3.2. Lithium isotopes

Lithium isotopic compositions were measured using a Neptune Multi Collector ICP-MS (Thermo Fischer Scientific).  $^7\text{Li}/^6\text{Li}$  ratios were normalized to the L-SVEC standard solution (NIST SRM 8545, Flesch et al. 1973) following the standard-sample bracketing method (see Millot et al. 2004 for more details). The analytical protocol involves the acquisition of 15 ratios with 16 s integration time per ratio, and yields in-run precision better than  $0.2\text{‰}$  ( $2\sigma_m$ ). Blank values are low, (i.e.  $0.2\text{‰}$ ), and 5 minutes wash time is enough to reach a stable background value.

The samples must be prepared beforehand with chemical separation/purification by ion chromatography in order to produce a pure mono-elemental solution. Chemical separation of Li from the matrix was achieved before the mass analysis following a procedure modified from the technique of James and Palmer (2000) using a cationic resin (a single column filled with 3 mL of BioRad AG® 50W-X12 resin, 200-400 mesh) and HCl acid media (0.2N) for 30 ng of Li. Blanks for the total chemical extraction were less than 30 pg of Li, which is negligible since it represents a  $10^{-3}$  blank/sample ratio.

Successful quantitative measurement of Li isotopic compositions requires 100% Li recovery. The column was, therefore, frequently calibrated and repeated analysis of the L-SVEC standard processed through columns shows 100% Li recovery and no induced isotope fractionation due to the purification process.

The accuracy and reproducibility of the entire method (purification procedure + mass analysis) were tested by repeated measurement of a seawater sample (IRMM BCR-403) after separation of Li from the matrix, for which we obtained a mean value of  $\delta^7\text{Li} = +31.1\text{‰} \pm 0.3$  ( $2\sigma$ ,  $n=11$ ) over the analysis period. This mean value is in good agreement with our long-term measurement ( $\delta^7\text{Li} = +31.0\text{‰} \pm 0.5$ ,  $2\sigma$ ,  $n=30$ , Millot et al. 2004) and with other values

reported in the literature (see, for example, Tomascak 2004 for a compilation). Consequently, based on long-term measurements of a seawater standard, we estimate the external reproducibility of our method to be around  $\pm 0.5\%$  ( $2\sigma$ ).

### 3.3. Boron isotopes

Boron isotopic compositions were determined on a Finnigan MAT 261 solid source mass spectrometer in a dynamic mode. For these samples, water volumes corresponding to a mass of 10  $\mu\text{g}$  of B underwent a two-step chemical purification using Amberlite IRA-743 selective resin according to a method adapted from Gaillardet and Allègre (1995). The boron aliquot sample (2  $\mu\text{g}$ ) was then loaded onto a Ta single filament with graphite, mannitol and Cs, and the B isotopes were determined by measuring the  $\text{Cs}_2\text{BO}_2^+$  ion (Spivack and Edmond 1986, 1987). The total boron blank is less than 10 ng. The values are given using the  $\delta$ -notation (expressed in ‰) relative to the NBS951 boric acid standard. The  $^{11}\text{B}/^{10}\text{B}$  of replicate analyses of the NBS951 boric acid standard after oxygen correction was  $4.04845 \pm 0.00104$  ( $2\sigma$ ,  $n = 19$ ) during this period. The reproducibility of the  $\delta^{11}\text{B}$  determination is then  $\pm 0.3\%$  ( $2\sigma$ ) and the internal uncertainty is better than  $0.3\%$  ( $2\sigma_m$ ).

The accuracy and reproducibility of the whole procedure were verified by the repeated measurements of the IAEA-B1 seawater standard (Gonfiantini et al. 2003) for which the mean  $\delta^{11}\text{B}$  value obtained is  $+39.21\% \pm 0.31$  ( $2\sigma$ ,  $n=20$ ), in agreement with the accepted value for seawater.

### 3.4. Strontium isotopes

Chemical purification of Sr ( $\sim 3 \mu\text{g}$ ) was done using an ion-exchange column (Sr-Spec) before mass analysis according to a method adapted from Pin and Bassin 1992, with total blank  $< 1$  ng for the entire chemical procedure. After chemical separation, around 150 ng of Sr was loaded onto a tungsten filament with tantalum activator and analysed with a Finnigan MAT 262 multi-collector mass spectrometer. The  $^{87}\text{Sr}/^{86}\text{Sr}$  ratios were normalized to an  $^{86}\text{Sr}/^{88}\text{Sr}$  ratio of 0.1194. An average internal precision of  $\pm 10$  ppm ( $2\sigma_m$ ) was obtained and the reproducibility of the  $^{87}\text{Sr}/^{86}\text{Sr}$  ratio measurements was tested by repeated analyses of the NBS987 standard, for which we obtained a mean value of  $0.710243 \pm 0.000022$  ( $2\sigma$ ,  $n=13$ ) during the period of analysis.

### 3.5. Uranium concentrations and isotopes

For U concentrations and isotope measurements, water samples were acidified to pH ~2 in order to avoid both metal adsorption on the container walls and bacteria development. They were then divided in two aliquots in the clean laboratory. Approximately 10% of the total sample was used for concentration measurements and was spiked with a double  $^{233}\text{U}$ - $^{236}\text{U}$  tracer.

U was co-precipitated with other transition metals using a Fe carrier and  $\text{NH}_4\text{OH}$ , following a standard procedure described in Chen et al. (1986). U chemical separation techniques have been described in detail elsewhere (Innocent et al. 2005).

Both U concentrations and  $^{234}\text{U}/^{238}\text{U}$  isotopic ratios were measured at BRGM on a Neptune MC-ICP-MS mass spectrometer equipped with an ion counter coupled with a retarding potential quadrupole (RPQ) filter.  $^{234}\text{U}$  was measured on the ion counter, whereas both spike isotopes and  $^{235}\text{U}$  and  $^{238}\text{U}$  were measured on Faraday cups. Samples were corrected, using the standard bracketing method, for a global measurement bias factor encompassing the mass fractionation and the yield of the ion counter. Such a correction makes it possible to eliminate sharp variations of the yield that may occur between the time of external calibration and the time of sample measurement. Moreover, this correction is justified by the fact that mass fractionation effects are reliably described using a linear law (Wasserburg et al. 1981), considering the uncertainty levels typical of U measurements (usually around 0.5%). When possible, the ion beam intensities measured by the ion counter were kept around  $10^4$  counts per second. The standard solution used for bracketing was the CRM U 010 standard ( $^{234}\text{U}/^{238}\text{U} = 5.4655 \cdot 10^{-5} \pm 9\text{‰}$ ,  $^{235}\text{U}/^{238}\text{U} = 0.01014 \pm 1\text{‰}$ ), provided by the New Brunswick Laboratory. Total blanks were lower than 250 pg.

### 3.6. Chemical geothermometry

The concentrations of most dissolved elements in thermal waters depend on the groundwater temperature and the weathered mineralogical assemblage (White 1965, Ellis 1970, Truesdell 1976, Arnórsson et al. 1983, Fouillac 1983). Since concentrations can be controlled by temperature-dependent reactions, they could theoretically be used as geothermometers to estimate the deep temperature of the water. However, to be used in this way, other conditions must be fulfilled (Fournier and Truesdell 1974, Michard 1979, Giggenbach 1981): 1 - Temperature-dependent reactions must occur at depth; 2 - The constituents involved must be sufficiently abundant (i.e. supply must not be a limiting factor); 3 - Water/rock equilibration must occur at the reservoir temperature; 4 - Little or no re-equilibration or change in composition must occur at lower temperatures as the water rises to the surface; 5 - The deep hot water must not mix with cooler shallow groundwater; 6 - There

must be no exchange reactions with argillaceous minerals, Na and K in particular (Weissberg and Wilson 1977).

Since 1965, several chemical and isotopic geothermometers have commonly been used in geothermal exploration (White 1965, 1970, Fournier 1979, Michard 1979, Giggenbach 1988, Nicholson, 1993, Serra and Sanjuan 2004). Traditional geothermometer equations (Fournier and Rowe 1966, Ellis 1970, Fournier 1973, 1977, 1979, Fournier and Truesdell 1973, Fournier and Potter 1979, Truesdell 1976, Giggenbach et al. 1983, Giggenbach 1988) include a silica geothermometer (based on quartz, chalcedony,  $\alpha$  or  $\beta$  cristobalite and amorphous silica solubility), a Na/K geothermometer (controlled by plagioclase and K-feldspar equilibrium) and a Na-K-Ca geothermometer (in the case of Ca-rich waters and that can include the Mg correction).

Unfortunately, the estimates of reservoir temperatures using these classical tools are not always in agreement, especially for low and moderate temperatures. This can be explained by different processes, including:

- chemical equilibrium reached for some of the fluid-reservoir rock reactions involving the geothermometers because these reactions are slower and longer at low and moderate temperatures than at high temperature
- mixing of the reservoir fluid with surface waters or seawater during its rise to the surface, which modifies its chemical composition
- cooling of the reservoir fluid and the associated precipitation/dissolution processes during its rise to the surface, which also modifies its chemical composition

Auxiliary chemical geothermometers were, therefore, developed, in particular those using lithium (Fouillac and Michard 1981, Kharaka et al. 1982, Michard 1990). Fouillac and Michard (1981) proposed two empirical and statistical Na/Li thermometric relationships depending on the salinity of numerous worldwide geothermal fluids in contact with crystalline rocks (essentially, volcanic rocks or granites). Using abundant data from geothermal wells throughout the world and US oil wells, Kharaka et al. (1982, 1985) and Kharaka and Mariner (1989) fitted this geothermometer for hot saline fluids (from 30 to 200°C) from sedimentary basins. They also developed a Mg/Li geothermometer for this type of fluids. Due to a low lithium reactivity during the rise of the geothermal reservoir fluid to the surface and under certain conditions, the use of the Na/Li geothermometer can give a more reliable estimation of the reservoir temperature than those obtained using the classical geothermometers, even though the way Na/Li geothermometer works is still poorly understood.

## **4. RESULTS AND COMMENTS**

### **4.1. Field data and elemental concentrations**

Physicochemical parameters (T, pH, Eh, conductivity) were measured in the field during sampling (Table 1). The data are only partial for Chaunoy water samples because conductivity could not be measured in the field due to the high groundwater temperature (> 50°C). For Champotran and La Torche, bulk samples were collected in the field (water + oil mixture), and measurements were done in the laboratory after the oil and water had been separated at room temperature. The major elements in these water samples (cations and anions) are given in Table 2. The dissolved salt content of Triassic formation waters varies greatly, with sodium concentrations between 55.1 mg/L and 52,000 mg/L and chloride concentrations between 12.7 mg/L and 102,000 mg/L. In general, water samples from Châteauroux and, to a lesser extent, Santenay are very dilute compared to water samples from Chaunoy, Champotran and La Torche. This is obvious when the chloride concentrations are plotted as a function of the sodium concentrations (Figure 2). In this graph, Triassic formation waters seem to define a linear correlation whose slope is slightly different from that representing only seawater dilution-evaporation processes. Brine waters from Chaunoy, Champotran and La Torche have Na and Cl concentrations higher than those of seawater. The brine sample from La Torche has the highest concentrations of both Cl and Na, brine samples from Chaunoy and Champotran have lower, but still relatively high, Cl and Na contents, and water samples from Santenay and Châteauroux are dilute. The low Cl and Na concentrations of the latter can be attributed to their location in the recharge area at the edge of the Paris Basin. These data are in agreement with literature data (Fontes and Matray 1993a, 1993b, Matray et al. 1994) (Figure 2). Concerning the other cation concentrations, those of K are between 7.9 and 1,954 mg/L, of Mg between 8.8 and 1,183 mg/L and of Ca between 20.1 and 8,339 mg/L.

The anion concentrations are also highly variable, depending on the sample type. Cl contents are between 12.7 and 102,000 mg/L, bromine concentrations are between < 0.1 and 990 mg/L, and sulphate concentrations vary from 26.6 to 2,479 mg/L. Dilute waters from Santenay have the highest sulphate contents (2,352 and 2,479 mg/L for Lithium and Santana, respectively).

It is well known that the Cl/Br ratio can be used to trace water origin (Rittenhouse 1967, Fontes and Matray 1993a). The Cl/Br ratios (w/w) for our water samples range between 103 for Chaunoy73 and 218 for Santana. All of the Triassic formation waters studied here have Cl/Br ratios lower than that of seawater (around 289). Our samples present a signature (Figure 3) that is compatible with a primary marine origin of the brine, which has evaporated at least up to the halite precipitation stage (decrease of the Cl/Br ratio due to Cl depletion). This figure was modified from Matray et al. (1989) and makes it possible to discern the

primary and secondary origins of brines using the Cl/Br relationship according to the Cl content.

In agreement with the literature data (Fontes and Matray 1993a, 1993b), the Keuper and Dogger formation brines are of primary origin, whereas those from Rhaetian formations are of secondary origin. In addition, waters from the Dogger formation are clearly dilute compared to those from the Triassic formation. Waters from Santenay are also very dilute because the boreholes are located on the edge of the sedimentary basin, near the recharge area.

Contrary to what is observed for cations and anions, the silica concentrations are less variable. SiO<sub>2</sub> concentrations range from 15.2 for GTH01 to 49.6 mg/L for Chaunoy73, which is approximately a factor of 3, whereas the cations vary by several orders of magnitude.

The trace elements concentrations in Triassic groundwaters (B, Li, Sr and U) are also highly variable (Table 2). Boron concentrations are between 0.32 and 120 mg/L. Lithium concentrations vary from 0.23 to 48 mg/L. Sr concentrations are between 0.85 and 495 mg/L. U concentrations are also highly variable, with concentrations ranging from 3.6 for Chaunoy73 to 4,525 ng/L for Santana.

Water samples from Chaunoy, Champotran and La Torche, and also those from Santenay (Lithium and Santana), have Li contents that are among the highest reported in the literature to date. For comparison, the Li-rich thermomineral water from Coren in the Massif Central (Millot and Négrel 2007) has a lithium concentration of 26.9 mg/L.

The waters sampled in this study are, therefore, of three different types: 1- seawater-derived brines (Na- and Cl-rich) in the centre of the Paris Basin (Chaunoy, Champotran and La Torche samples), 2- thermo-mineral waters (Na-, Cl- and SO<sub>4</sub>-rich) in the Santenay region (Santana and Lithium samples), and 3- dilute (or fresh) water in the recharge zone (Châteauroux sample).

#### **4.2. Stable isotopes of the water molecule: $\delta D$ and $\delta^{18}O$**

The  $\delta D$  and  $\delta^{18}O$  values for Triassic formation waters are given in Table 3.  $\delta D$  values range between -55.6 and -7.6‰ (vs. SMOW), whereas  $\delta^{18}O$  values are comprised between -8.3 and -0.9‰ (vs. SMOW). Figure 4a shows a graph of  $\delta D$  vs.  $\delta^{18}O$  values for Triassic formation waters from this study on which we have also plotted literature values for  $\delta D$  and  $\delta^{18}O$  for Dogger formation waters (Fontes and Matray 1993a, Marty et al. 2003), Rhaetian and Keuper formation waters (Fontes and Matray 1993a), and brines from Keuper formations (Varangéville, Fontes and Matray 1993b). The brines from the eastern part of the basin (Marty et al. 2003) have low  $\delta D$  and  $\delta^{18}O$  values near the Global Meteoric Water Line

(GMWL,  $\delta D = 8 \times \delta^{18}O + 10$ , Craig 1961). Their mean value is, moreover, similar to that of the modern input signal (-62 and -9‰, respectively, for  $\delta D$  and  $\delta^{18}O$ , Matray et al. 1989). The other data from Rhaetian and Keuper formation waters (Fontes and Matray 1993a, 1993b) lie to the right of the GMWL, indicating that there has been evaporation or a mixing of different waters in the reservoir.

Our water samples are located on or near the GMWL. This is particularly true for the Châteauroux water sample (GTH01) and the Santenay waters (Lithium and Santana). The other samples have less-negative  $\delta D$  and  $\delta^{18}O$  values, slightly to the right of the GMWL and significantly different from modern seawater (as represented by the SMOW standard). Figures 4b and 4c ( $\delta D$  and  $\delta^{18}O$  vs. Cl concentrations) indicate good correlation between Cl concentrations and  $\delta D$  and  $\delta^{18}O$  values ( $\delta D = 5.0 \times 10^{-4} \times Cl - 55.42$ ,  $R^2=0.99$  and  $\delta^{18}O = 8.0 \times 10^{-5} \times Cl - 8.29$ ,  $R^2=0.99$ ). This suggests that our water samples are essentially derived from a primary marine brine that evaporated, at least up to the halite precipitation stage and was then diluted, in various proportions, by meteoric waters that give  $\delta D$  and  $\delta^{18}O$  signatures (-58 and -9‰, respectively) close to the modern input signal. This hypothesis is in good agreement with the investigation of Cl/Br ratios (Figure 3).

These trends are probably related to the recharge effect. When  $\delta^{18}O$  values in water samples are plotted according to the estimated distance from the recharge zone (Figure 4d), there is a good correlation ( $\delta^{18}O = 2.66 \times 10^{-5} \times \text{distance} - 8.48$ ,  $R^2=0.97$ ).

### 4.3. Strontium isotopes

Strontium isotopic ratios for Triassic formation waters are reported in Table 3. Whereas Sr concentrations vary between 0.85 and 495 mg/L (for Châteauroux and La Torche, respectively),  $^{87}\text{Sr}/^{86}\text{Sr}$  ranges from 0.710432 (La Torche) to 0.715974 (Santana).

If we compare the results obtained for Sr isotopes for these waters to the various known sources of Sr in groundwaters (Figure 5) and to literature data, we observe that waters from the Paris Basin present strong variations in their isotopic signatures of Sr (0.710-0.716). Saline waters from Chaunoy, Champotran and La Torche have the highest Sr contents and Sr isotopic ratios of around 0.710-0.711. On the other hand, the values obtained for dilute waters from Santenay (0.7158-0.7159) show a more radiogenic contribution. In general, these  $^{87}\text{Sr}/^{86}\text{Sr}$  values indicate a water signature having interacted with sedimentary lithologies (Figure 5). Furthermore, these Sr isotopes signatures are higher than  $^{87}\text{Sr}/^{86}\text{Sr}$  ratios reported for Triassic seawater (0.7074-0.7079, Burke et al. 1982; Koepnick et al. 1990).

Finally, following Matray et al. 1989, Dogger formation waters have typically marine Sr isotopic ratios ( $0.7072 < {}^{87}\text{Sr}/{}^{86}\text{Sr} < 0.7082$ ) indicating exchanges with a carbonate reservoir.

#### 4.4. Lithium isotopes

Lithium isotopic ratios for Triassic formation waters are given in Table 3. The lithium concentrations in these water samples are highly variable, ranging between 0.23 mg/L (Châteauroux) and 48.0 mg/L (La Torche).  $\delta^7\text{Li}$  values (‰) for Triassic formation waters are comprised between +6.7‰ (Châteauroux) and +10.9‰ (La Torche). This range of variation is in agreement with data reported for other groundwater samples by Millot et al. (2007) and Millot and Négrel (2007).

The lithium isotopic compositions were plotted against the Li concentration (Figure 6) and we observe that, for Triassic formation waters,  $\delta^7\text{Li}$  value tends to decrease when the Li concentration increases, although La Torche water does not follow this general trend.

Lithium isotope data obtained for Triassic formation waters in the Paris Basin can only be compared with values measured for carbonated formation waters from the Dogger formation sampled in the Eastern part of the Paris Basin. These water samples were collected at the Meuse/Haute-Marne Site and analysed within the ISOBLiFe project funded jointly by BRGM and ANDRA (French National Radioactive Waste Management Agency, Girard et al. 2006).

Dogger and Triassic formation waters have very different lithium concentrations and isotopic signatures. The lithium isotopic signatures of Triassic formation waters are systematically lower than those of the Dogger formation waters. It is also noteworthy that the  $\delta^7\text{Li}$  values of the Triassic formation waters are very different from those of modern seawater (i.e.  $\delta^7\text{Li} = +31.0\text{‰}$ , Millot et al. 2007).

#### 4.5. Boron isotopes

Boron isotopic ratios for Triassic formation waters are given in Table 3. Whereas boron concentrations vary from 0.32 mg/L (Châteauroux) to 120 mg/L (La Torche), boron isotopic ratios range from +5.1‰ (Santana) to +25.5‰ (Chaunoy73). This range of variation is in agreement with literature data for groundwaters (Mossadik 1997, Millot et al. 2007, Millot and Négrel 2007, Williams et al. 2001b).

$\delta^{11}\text{B}$  values (‰) for Triassic formation waters were plotted alongside those measured by Mossadik (1997) for Keuper and Dogger formation waters (waters from oil-bearing formations and geothermal fields) and the Dogger formation waters sampled in the East of the Paris Basin (Girard et al. 2006) (Figure 7). We see that our data for Triassic formation

waters agree well with literature data (Mossadik 1997). However, water samples from Châteauroux (GHT01) and Santenay (Lithium and Santana) seem to be very peculiar when  $\delta^{11}\text{B}$  values are plotted as a function of B concentration. Indeed, GTH01 has the lowest B concentration and both Lithium and Santana water samples have the lowest  $\delta^{11}\text{B}$  values.

#### 4.6. Uranium isotopes

Uranium isotopic ratios for Triassic formation waters are given in Table 3. Both uranium concentrations and  $^{234}\text{U}/^{238}\text{U}$  activity ratios are highly variable. U concentrations range from 3.6 to 4,525 ng/L (Table 2) and  $^{234}\text{U}/^{238}\text{U}$  activity ratios range from  $1.14 \pm 0.02$  (La Torche) to  $9.64 \pm 0.02$  (Santana). However, it should be stressed that the highest U contents are recorded in the two Santenay waters, whereas U concentrations are much lower and remain more or less in the same range for the other samples (Châteauroux and samples from Chaunoy, Champotran and La Torche in the centre of the basin). Moreover, the average value that can be calculated for waters in the centre of the basin is 31.4 ng/L, which is close to the Châteauroux value (recharge area).

The highest activity ratios are measured in the Santenay waters (8.912 and 9.637, respectively for Lithium and Santana), but the Châteauroux sample (GTH01) also displays a high  $^{234}\text{U}/^{238}\text{U}$  activity ratio of 6.064. Finally, as indicated in Table 3 and Figure 8, waters from Chaunoy, Champotran and La Torche have clearly lower ( $^{234}\text{U}/^{238}\text{U}$ ) values, ranging from 1.138 to 1.935. Similarly to U contents, activity ratios in the centre of the basin are much lower than for Châteauroux, and are very variable with an average value around 1.41 (Chaunoy, Champotran and La Torche).

These heterogeneities in U contents and activity ratios for the waters located in the centre of the basin could be possibly attributed to the fact that they are oil-bearing waters. However, it is important to note that water samples from the centre of the basin do not reach secular equilibrium.

## 5. DISCUSSION

### 5.1. Chemical geothermometry

The results of the application of the principal geothermometers to the Triassic formation waters sampled and analysed during this study are presented in Table 4.

#### 5.1.1. Waters from Chaunoy, Champotran and La Torche (saline waters)

Whereas, water samples from the Chaunoy and Champotran boreholes have high salinities (around 120 g/L) and similar chemical compositions, the salinity of the La Torche water sample is significantly higher (168 g/L). However, for all of these waters sampled in the oil-bearing fields in the centre of the Paris Basin, we observe that the SiO<sub>2</sub>-Quartz (Fournier and Rowe 1966) or Chalcedony (Helgeson et al. 1978), Na/K (Michard 1979), Na/K/Ca/Mg (Fournier and Potter 1979) and Na/Li (Fouillac and Michard 1981) geothermometers give similar temperature values between 80 and 100°C (Table 4). These temperatures are in agreement with the evolution curves of both the subsidence and the temperature of the Paris Basin through time reported by Worden et al. (1999). They also imply that the Triassic fluids are at equilibrium, under the current temperature conditions, with the minerals constituting the reservoir rocks.

According to Azaroual et al. (1997), the dissolved silica concentrations in Triassic formation waters (Keuper) correspond to a thermodynamic equilibrium of these fluids with both quartz (observed in diagenetic cements) and chalcedony. This is in agreement with our results and the saturation state of these waters with respect to quartz and chalcedony at 100°C calculated in this study (Table 5) using the EQ3NR code (Wolery 1995). In addition, the good results obtained using the Na/K geothermometer, at relatively low temperature (100°C), may be explained by the calculated saturation of these waters with respect to K- and Na-feldspar, which are two mineral phases also observed in diagenetic cements related to the basin evolution (Azaroual et al. 1997, Worden et al. 1999). The saturation indices calculated at 100°C for the Chaunoy waters (Table 5) suggest that the Triassic brines are also in equilibrium with various clays (muscovite, which can be thermodynamically considered to be the pure end-member of K-illite, montmorillonite, Rosenberg and Kittrick 1990, Sanjuan et al. 2003), carbonate minerals (calcite, disordered dolomite and strontianite) and sulphate minerals (anhydrite and barite). These results are in good agreement with the petrographical and mineralogical observations made on the diagenetic cements of the Triassic reservoirs, which are characterized by a single diagenetic sequence (Matray et al. 1989, Azaroual et al. 1997, Worden et al. 1999). This diagenetic sequence is constituted mainly of dolomicrite and dolosparite cement, quartz, anhydrite cement and, in places, reprecipitated anhydrite, plagioclase and dissolved K-feldspar and several stages of neoformed illite, which are observed, in places, as the last diagenetic episode.

The relatively concordant results obtained using the Na/Li geothermometer (Fouillac and Michard 1981) are more difficult to understand here because this relationship can generally be applied only to waters having chloride concentrations lower than 0.3 mol/L (which is not the case here). In theory, the Na/Li geothermometer (Kharaka et al. 1982, Table 4), based on and developed using data collected on sedimentary and oil basins, should give the best temperature estimates. One of the explanations for this over-estimate of temperature

systematically observed using this relationship (around 140-150°C) could be the existence of abnormally high concentrations of lithium in these fluids. It is likely that these high lithium concentrations could be explained by a warmer episode in the past (major subsidence of the basin, as proposed by Worden et al. 1999), which would not have had time to be rebalanced under the current temperature conditions.

In addition, the Mg/Li geothermometer generally used for sedimentary basins and oil-fields (Kharaka and Mariner 1989) also over-estimates temperatures values compared to the current temperature conditions (Table 4).

#### *5.1.2. Waters from Santenay and Châteauroux (dilute waters)*

For the Santenay and Châteauroux water samples, only a few geothermometers can be used because these are shallow groundwaters and very dilute compared to other Triassic formation waters (especially Châteauroux). For the Châteauroux groundwater, SiO<sub>2</sub>-Quartz (Fournier and Rowe 1966) or Chalcedony (Helgeson et al. 1978) and Na/K/Ca/Mg (Fournier and Potter 1979) geothermometers converge around a temperature of 45°C (Table 4). For the Santenay groundwaters, whose chemical compositions are almost identical, only the temperature of around 40-50°C estimated using the SiO<sub>2</sub>-Quartz (Fournier and Rowe 1966) or Chalcedony (Helgeson et al. 1978) geothermometer seems to be suitable (Table 4).

These results and the calculation of the saturation indices using the EQ3NR code (Table 5) seem to show that there are few reactions at equilibrium between these waters and the aluminosilicate minerals in the surrounding rocks. We can conclude that because these dilute waters are near the recharge zone and are shallow (compared to saline waters), they are subjected to relatively low temperatures and high fluid circulation rates, neither of which facilitates advanced water/rock interactions. These waters seem, however, to be in equilibrium (Table 5) with some carbonate minerals (calcite, disordered dolomite, strontianite, siderite) or sulphate minerals (anhydrite, barite).

#### **5.2. Multi-isotopic characterization of deep Triassic formation waters (Li-B-Sr isotopes)**

Lithium, boron and strontium isotopes were systematically coupled in X-Y diagrams (Figure 9) in a multi-isotope approach, in order to attempt to i) identify the different sources contributing to the Li-B-Sr isotopic signature and ii) determine the main processes controlling these isotopic compositions for the Triassic formation waters.

Sr isotopes were studied in order to better define the signature of the reservoir the waters came from, given that Sr isotopes in water reflect the origin of water/rock interactions

(Goldstein and Jacobsen 1987, Négrel et al. 1997, Négrel 1999, Négrel et al. 2000). It is well accepted that the Sr isotopic composition of water is a good tracer of the reservoir source, since the Sr isotopic composition of a groundwater is the fingerprint of the isotopic composition of the bedrock with which it has interacted. Lithium and boron isotopic compositions ( $\delta^7\text{Li}$  and  $\delta^{11}\text{B}$ ) were also studied in an attempt to provide additional constraints on the origin of Li and B in these waters.

The different fields in figure 9 correspond to the principal lithologies that could have contributed to the Li-B-Sr isotopic signatures of these waters during water/rock interactions (see the figure caption for references). The fields for Li and B (Millot et al. 2010a), and Sr (Négrel et al. 2007) isotopic signatures in French rainwaters are also shown in the figure, considering that rainwater sampled in Orléans is representative of the continental meteoric input (see figure 1 for the location of Orléans). The Li-B-Sr isotopic signatures of Dogger formation waters (Girard et al., 2006) are also shown in the figure, for comparison.

Figure 9 shows that: i) Triassic formation waters from the centre of the Paris Basin (Chaunoy and Champotran) have similar Li-B-Sr isotopic signatures, ii) water samples from La Torche have Li-B-Sr isotopic signatures that are slightly different from other waters from oil-bearing fields in the centre of the basin, whereas iii) waters sampled near the recharge zones have very different Li-B-Sr isotopic signatures compared to the others (especially obvious for Santenay waters).

More specifically, the Li-B-Sr isotopic signatures of the deep fluids in the centre of the Paris basin are in agreement with waters resulting from water/rock interactions involving a mixture of meteoric water and seawater-derived brine (Figure 9). It is also very likely that the isotopic signatures for Chaunoy, Champotran and La Torche waters also reflect a contribution derived from sandstones, as this type of rock constitutes the main rock reservoir from which these fluids are derived during water/rock interactions. Unfortunately, few isotope data are available for this type of rock to date in the literature. Nevertheless, Teng et al. (2004) have reported a range of  $\delta^7\text{Li}$  values between -3.2 and +5.2‰ for shales, and Millot et al. (2007) have reported  $\delta^7\text{Li}$  and  $^{87}\text{Sr}/^{86}\text{Sr}$  ratios of -4‰ and 0.7175, respectively, for a sandstone rock from the French Massif Central. For strontium, this means that the signature derived from the sandstone reservoir is radiogenic. This is in agreement with our Sr isotope data (Figs. 9a and 9b), where Triassic formation waters have Sr isotope ratios higher than the mean carbonate signature of the Jurassic reservoir.

Concerning lithium, the study of  $\delta^7\text{Li}$  values in Triassic formation waters raises the question of the origin of the lithium in these waters (Figs. 9b and 9c). Several hypotheses were proposed by Fontes and Matray (1993b) for the origin of the high lithium concentrations in Triassic formation waters: diagenesis effects, halite dissolution, global or local enrichment of

Triassic seawater, and a primary (highly concentrated) brine contribution. Worden et al. (1999) also remarked on the abnormally high concentrations of lithium in these fluids and suggested that they might be explained by a warmer episode in the past (major subsidence of the basin).

Several studies of Li-isotope behaviour in weathering environments have shown that  $\delta^7\text{Li}$  values do not directly reflect the lithology, but instead are controlled by fractionation during water/rock interactions (Huh et al. 1998, 2001, 2004, Pistiner and Henderson 2003, Kusakürek et al. 2004, 2005, Pogge von Strandmann et al. 2006, Vigier et al. 2009, Lemarchand et al. 2010, Millot et al. 2010b). It has been suggested that the  $\delta^7\text{Li}$  signature in the liquid might be controlled by the preferential retention of  $^6\text{Li}$  in secondary mineral phases during the weathering processes. It has also been shown that the fractionation of lithium isotopes during water/rock interaction also depends on temperature because different secondary minerals might control the uptake or release of Li in secondary minerals depending on the temperature of interaction and the associated dissolution/precipitation reaction (Chan and Edmond 1988, Chan et al. 1992; 1993; 1994; Chan et al. 2002). In a recent study of water/rock interactions for temperature ranging from 25 to 250°C, we experimentally determined a relationship between the Li isotopic fractionation (between the solution and the solid) and temperature ( $\Delta_{\text{solution} - \text{solid}} = 7847 / T(\text{K}) - 8.093$ , Millot et al. 2010c). Using this equation, deep Triassic formation waters having temperatures in the 80-100°C range would correspond to Li isotopic fractionation  $\Delta_{\text{solution} - \text{solid}}$  values of between 12.2 and 13.4‰ for 100 and 80°C, respectively. Considering the  $\delta^7\text{Li}$  values in the Triassic formation waters (+6.7 to +10.9‰), we can conclude that for the fractionation of Li isotopes at these temperatures, we can obtain  $\delta^7\text{Li}$  in rock reservoirs that are in agreement with values reported for clastic rocks (-4‰, Millot et al. 2007) and  $\delta^7\text{Li}$  values reported for shales (-3.2 and +5.2‰, Teng et al. 2004). In addition, the hypothesis proposed above of a warmer episode in the past can be confirmed because it would lead to lower fractionation between the solution and the solid ( $\Delta_{\text{solution} - \text{solid}}$  values comprised between 10.0 and 11.1‰ for 140 and 120°C, respectively), compatible with  $\delta^7\text{Li}$  values reported for clastic rocks in the literature.

The same approach can be used for boron isotopes. Using the equation proposed by Williams et al. (2001a),  $\Delta_{\text{solution} - \text{solid}} = 10120 / T(\text{K}) - 2.44$ , we calculate B isotopic fractionation  $\Delta_{\text{solution} - \text{solid}}$  values comprised between 24.7 and 26.2‰ for 100 and 80°C, respectively. This high isotopic fractionation reflects mainly the illitization process occurring during diagenesis, and considering the  $\delta^{11}\text{B}$  values for deep Triassic formation water in the central part of the Paris Basin (from +22.5 to +25.5‰) and the fractionation values that we

obtained, we can conclude that the B isotope data are compatible with the boron isotope compositions reported by Williams et al. (2001b) for sandstones.

Li and B isotopes signatures for deep Triassic formation waters are, therefore, in a good agreement with a fluid signature derived mainly from water/rock interactions involving silicate minerals (clastic rocks) with water essentially resulting from a seawater-derived brine endmember diluted by meteoric waters.

### **5.3. Residence time of waters within the Triassic aquifer (U isotopes)**

U isotope data might constrain estimates of the residence time of water in the Triassic aquifer, in terms of both mean groundwater flow velocity (m/yr) and age (My). We have seen (section 4.6.) that the highest U activity ratios are found in the vicinity of the recharge area at the edge of the sedimentary basin (Santenay and Châteauroux). Santenay water samples are slightly reducing or, at least, non-oxidizing (Eh = -8 and -10 mV for Lithium and Santana, respectively), whereas the Châteauroux water sample is clearly reducing (Eh = -120 mV). The Santenay water is probably located at or near a redox barrier as the U concentrations increase as we move away from this area (Coward 1980). The very high  $^{234}\text{U}/^{238}\text{U}$  activity ratios for Santenay and Châteauroux might be caused by the presence of dolomitic facies in these two areas (Hamon 2001), or the enrichment in  $^{234}\text{U}$  might be the result of the percolation of recharge water through the ground. These two possible causes are not exclusive.

Since water samples from the oil-bearing fields located in the centre of the aquifer are strongly reducing, we can test the simple model of Ivanovitch et al (1991) for the asymptotic disintegration of  $^{234}\text{U}$  from a redox barrier to reducing waters. This allows us to calculate an average apparent velocity of fluid circulation of about 0.25 m/yr (curve #1, Figure 10). The high U concentrations measured in the two Santenay waters may challenge this result, as the model does not take into account possible gain and/or loss of U due to water/rock exchange processes. However, the same calculation, carried out considering only the Châteauroux water and the average characteristics of the waters from the centre of the basin (Chaunoy, Champotran and La Torche) results in a comparable average velocity of 0.2 m/yr (curve #2, Figure 10).

It is noteworthy that the two sample waters from Santenay plot also on curve #2 in Figure 10. This could indicate that most U is lost at the redox barrier (Ivanovitch et al. 1991). If no incoming U is trapped, this will not modify the activity ratio. Alternatively, the fact that the Santenay data points plot more or less on that curve can be purely fortuitous. Indeed, Santenay waters are shallow thermo-mineral waters that can be not representative of U behaviour in the deep aquifer. Moreover, they display Sr isotopic signatures that are much

higher than the other waters. At present, we have no further argument to decipher between these two possibilities. Once said, it is noteworthy that such high activity ratios like those measured in Santenay waters, though not very rare, are in any case somewhat unusual.

The average apparent velocity of fluid circulation is about 0.2 m/yr (curve #2 in Figure 10) and suggests an age close to 1.25 My for the waters from the oil-bearing fields in the centre of the Paris Basin (Chaunoy, Champotran and La Torche). This is in agreement with the study of Pinti and Marty (1995), who reported rare gas isotope compositions of oil from the East of the Paris Basin and also constrained the water/oil interactions in the Triassic aquifer. Pinti and Marty (1995) thus estimated residence times for Triassic waters in the My range.

On the other hand, the mean apparent velocity of fluid circulation calculated using uranium activity ratios (0.2 m/yr) is much lower than those published by Blavoux and Olive (1981) and Marty et al. (2003). These two studies were carried out on waters sampled close to the main recharge zone in Lorraine (East of the Paris Basin). Blavoux and Olive (1981) reported a mean apparent fluid circulation velocity of 1.9 m/yr depending on the physical parameters of the aquifer (permeability, diffusivity), but also noted that the ages determined for these waters could be a sign of much lower fluid circulation velocities. Moreover, Marty et al. (2003) showed, by analyzing waters from the same zone, that the mean apparent fluid circulation velocity could be about  $3.7 \pm 1.3$  m/yr, with calculated ages lower than 30 kyr. Blavoux and Olive (1981) also observed that the hydraulic gradient can vary not only in space (permeability variations), but also in time (climate variations).

The advantage of uranium isotopes is that the half-life of the nuclide  $^{234}\text{U}$  (248 kyr) makes it possible to smooth these variations, which is of interest because the time spans are too short to be recorded by this system. It is, therefore very likely that the average velocity over a 1 My time span is lower than that currently measured on the basis of  $^{14}\text{C}$  data, as suggested by Blavoux and Olive (1981). Indeed, a flow rate of 3 m/yr, for example, would result in  $^{234}\text{U}/^{238}\text{U}$  activity ratios much higher than those measured for water samples from the oil-bearing fields (Chaunoy, Champotran and La Torche).

Rare gas isotope studies that focused on two boreholes in the Triassic aquifer (Melleray and Céré-la-Ronde, Castro and Jambon 1998, Castro et al. 1998) concluded that Triassic formation waters could be very old (15 to 30 My) when located at the centre of the aquifer. However, these studies show also that the rare gases are vertically transported in a massive way from the subjacent base towards the aquifer, which can lead to incoherent ages, as the authors already mentioned (Castro and Jambon 1998). Such old ages would consequently imply that the  $^{234}\text{U}$  and  $^{238}\text{U}$  activities should be at secular equilibrium in these waters, unless we consider a contribution of uranium with an activity ratio higher than 1. In addition, this input should be constant at the scale of ten million years.

Waters from the overlying Dogger aquifer could be a possible candidate. However, an input from Dogger groundwaters is unlikely, since an opposite migration of brines from the Triassic aquifer to the Dogger aquifer has been evidenced (Matray et al. 1994). Moreover, Sr isotopes do not favor at all the hypothesis of an input from Dogger waters.

The use of the model proposed by Ivanovitch et al. (1991) could be considered to be too simple. However, it should be kept in mind that, as all water samples from the centre area come from 3 sites that are very close to each other, the interpretation of U data as a global geographic scale (the whole Paris Basin) holds finally only on 2 or 3 points, whether Santenay waters are included or not. Hence it is difficult to take into account the possible gain and/or loss of U due to water/rock interaction as well as the  $\alpha$  recoil effect on such a restricted dataset. Furthermore, it is not sure at all that more complex modelling could bring significant additional information. Nevertheless, some solid hypotheses can be drawn from this simple model on average residence times for Triassic formation waters. Obviously, they have to be considered with a certain caution pending additional data that could be derived from new deep boreholes which will be drilled in the future.

## 6. CONCLUSIONS

The present work has made it possible to better characterize Triassic formation waters by the combined use of chemical and multi-isotope studies as well as by the use of chemical geothermometers for temperature estimates. For this study, four samples were collected in the central part of the Paris Basin (Chaunoy, Champotran and La Torche), and three were collected at the edge of the basin (Châteauroux and Santenay). The principal results of this study are:

- The saline waters collected from the Chaunoy and Champotran boreholes in the centre of the Paris basin, have high salinities (around 120 g/L) and very similar chemical and isotopic compositions. The La Torche water sample has a significantly higher salinity (168 g/L) and considerably different isotope characteristics (hydrogen, oxygen, lithium and boron isotopes). The chemical geothermometers applied to these fluids give temperature values of ranging from 80 to 100°C.
- The water samples from locations on the edge of the basin (Santenay and Châteauroux) have very different chemical and isotopic compositions. These dilute water samples come from shallow depths with colder temperatures around 45 to 50°C.
- The study of the uranium activity ratio vs. the distance to the recharge zone makes it possible, as a first approximation, to suggest a mean apparent fluid circulation velocity of approximately 0.2 m/yr, which would correspond to a “mean age” of approximately 1.25 My

for water sampled in the Chaunoy, Champotran and La Torche fields in the centre of the Paris Basin.

- The multi-isotope characterization of deep Triassic formation waters shows that (i) our data are in agreement with those from the literature as concerns “traditional” isotope systematics: stable isotopes of the water molecule (oxygen and hydrogen), strontium isotopes, and that (ii) Li and B isotope signatures in the centre of the Paris basin are in a good agreement with a fluid signature derived mainly from water/rock interactions involving clastic rocks with water essentially resulting from a seawater-derived brine endmember diluted by meteoric waters. The data reported in the present work for Li and B isotopes could be used as a reference for future studies to characterize sandstone formation waters.

## **Acknowledgements**

This work was funded within the framework of a research partnership between BRGM and ADEME (Ph. Laplaige) and, more specifically, through the CLASTIQ project (CLAYed sandSTone In Question). We would like to thank V. Bouchot, A. Gadalia and M. Azaroual for fruitful discussions. We also would like to thank M. Brach, A. Brenot, C. Fléhoc, G. Négrel, R. Koopmann and T.D. Bullen for their help in collecting samples. This work benefited from the collaboration of BRGM Chemistry laboratories for the major and trace elemental analyses: J.P. Ghestem, T. Conte and C. Crouzet are thanked for their help, as well as C. Fléhoc for stable isotopes measurements ( $\delta\text{D}$  and  $\delta^{18}\text{O}$ ). We also would like to thank M. Robert for her help in the Neptune laboratory. We cordially thank P. Monget (Vermilion Emeraude) for his assistance and for access to the oil fields (Chaunoy, Champotran and La Torche). We thank CFG Services (French Company of Geothermics) for permission to sample the Châteauroux well. We also wish to thank E. Soncourt (ANTEA) for sharing unpublished data concerning boreholes in Santenay. We also thank ANDRA (French Agency for Radioactive Waste Management) for sharing unpublished data on Dogger formation waters. Lastly, we thank Mr. Mayor of Santenay who allowed us to collect water from two boreholes (Lithium and Santana). We thank two anonymous reviewers for providing critical comments that improved this manuscript. B. Bourdon is also thanked for editorial handling and constructive comments. This is BRGM contribution n° 6904.

## References

- Arnórsson S., Gunnlaugsson E., Svavarsson H. (1983) The geochemistry of geothermal waters in Iceland. III. Chemical geothermometry in geothermal investigations. *Geochim. Cosmochim. Acta*, 47: 567-577.
- Azaroual M., Fouillac C., Matray J.M. (1997) Solubility of silica polymorphs in electrolyte solutions: II. Activity of aqueous silica and solid silica polymorphs in deep solutions from the sedimentary Paris Basin. *Chem. Geol.*, 140: 167-179.
- Barth S.R. (1993) Boron isotope variations in nature: a synthesis. *Geol. Rundsch*, 82: 640-641.
- Barth S.R. (2000) Geochemical and boron, oxygen and hydrogen isotopic constraints on the origin of salinity in groundwaters from the crystalline basement of the Alpine Foreland. *Applied Geochemistry*, 15: 937-952.
- Blavoux B., Olive P. (1981) Radiocarbon dating of groundwater of the aquifer confined in the Lower Triassic sandstones of the Lorraine region, France. *Journal of Hydrology*, 54: 167-183.
- Bouchot V., Bialkowski A., Lopez S., Ossi A. (2008) Evaluation du potentiel géothermique des réservoirs clastiques du Trias du Bassin de Paris. Rapport final BRGM - RP-56463-FR, 92 p.
- Burke W.H., Denison R.E., Hetherington E.A., Koepnick R.B., Nelson H.F., Otto J.B. (1982) Variation of seawater  $^{87}\text{Sr}/^{86}\text{Sr}$  throughout Phanerozoic time. *Geology*, 10: 516-519.
- Casanova J., Girard J.P., Guerrot C., Innocent C., Millot R., Motelica M. (2006) Caractérisation isotopique (B, Li, U, Th, Fe) des eaux de forages scientifiques du site de Meuse/Haute-Marne. BRGM/RP-54310-FR, 60 p.
- Castro M.C., Jambon A. (1998) Noble gases as natural tracers of water circulation in the Paris Basin. 1. Measurements and discussion of their origin and mechanisms of vertical transport in the basin. *Water Resources Research*, 34: 2443-2466.
- Castro M.C., Goblet P., Ledoux E., Violette S., de Marsily G. (1998) Noble gases as natural tracers of water circulation in the Paris Basin. 2. Calibration of a groundwater flow model using noble gas isotope data. *Water Resources Research*, 34: 2467-2483.
- Chan L.H. and Edmond J.M. (1988) Variation of lithium isotope composition in the marine environment: A preliminary report. *Geochimica et Cosmochimica Acta*, 52, 1711-1717.
- Chan L.H., Edmond J.M., Thompson G., Gillis K. (1992) Lithium isotopic composition of submarine basalts: implications for the lithium cycle in the oceans. *Earth and Planetary Science Letters*, 108, 151-160.

- Chan L.H., Edmond J.M., Thompson G. (1993) A lithium isotope study of hot springs and metabasalts from mid-ocean ridge hydrothermal systems. *Journal of Geophysical Research*, 98, 9653-9659.
- Chan L.H., Gieskes J.M., You C.F., Edmond J.M. (1994) Lithium isotope geochemistry of sediments and hydrothermal fluids of the Guaymas Basin, Gulf of California. *Geochimica et Cosmochimica Acta*, 58, 4443-4454.
- Chan L. H., Alt J.C., Teagle D.A.H. (2002) Lithium and lithium isotope profiles through the upper oceanic crust: a study of seawater-basalt exchange at ODP Sites 504B and 896A. *Earth and Planetary Science Letters*, 201, 187-201.
- Chen J.H., Edwards R.L., Wasserburg G.J. (1986)  $^{238}\text{U}$ ,  $^{234}\text{U}$  and  $^{230}\text{Th}$  in seawater. *Earth and Planetary Science Letters*, 80: 241-251.
- Cowart J.B. (1980) The relationship of uranium isotopes to oxidation/reduction in the Edwards carbonate aquifer of Texas. *Earth and Planetary Science Letters*, 48: 277-283.
- Craig H. (1961) Isotopic variations in meteoric waters. *Science*, 133: 1702-1703.
- Ellis A. J. (1970) Quantitative interpretations of chemical characteristics of hydrothermal systems. *Geothermics Special Issue*, 2: 516-528.
- Flesch G.D., Anderson A.R., Svec H.J. (1973) A secondary isotopic standard for  $^6\text{Li}/^7\text{Li}$  determinations. *International Journal of Mass Spectrometry and Ion Physics*, 12: 265-272.
- Fontes J.Ch., Matray J.M. (1993a) Geochemistry and origin of formation brines from the Paris Basin, France. 2 Saline solutions associated with oil fields. *Chemical Geology*, 109: 177-200.
- Fontes J.Ch., Matray J.M. (1993b) Geochemistry and origin of formation brines from the Paris Basin, France. 1 Brines associated with Triassic salts. *Chemical Geology*, 109: 149-175.
- Fournier R.O. (1973) Silica in thermal water: Laboratory and field investigations. In: *Proceedings of the International Symposium on Hydrogeochemistry and Biogeochemistry, Japan, 1970: Vol. 1, Washington, DC, The Clark Company*, 122-139.
- Fournier R.O. (1977) Chemical geothermometers and mixing models for geothermal systems. *Geothermics*, 5: 41-50.
- Fournier R.O. (1979) A revised equation for the Na/K geothermometer. *Geoth. Res. Council Trans.*, 3: 221-224.
- Fournier R.O., Rowe J.J. (1966) Estimation of underground temperatures from the silica content of water from hot springs and wet-steam wells. *American Journal of Science*, 264: 685-697.
- Fournier R.O., Truesdell A.H. (1973) An empirical Na-K-Ca geothermometer for natural waters. *Geochim. Cosmochim. Acta*, 37: 1255-1275.

- Fournier R.O., Truesdell A.H. (1974) Geochemical indicators of subsurface temperature— Part 2, Estimation of temperature and fraction of hot water mixed with cold water. *Jour. Research U.S. Geol. Survey*, 2: 263-270.
- Fournier R.O., Potter R.W. (1979) Magnesium correction to the Na-K-Ca chemical geothermometer. *Geochim. Cosmochim. Acta*, 43: 1543-1550.
- Fouillac C. (1983) Chemical geothermometry in CO<sub>2</sub>-rich thermal waters. Example of the French Massif central. *Geothermics*, 12: 149-160.
- Fouillac C., Michard G. (1981) Sodium/Lithium ratio in water applied to geothermometry of geothermal reservoirs. *Geothermics*, 10: 55-70.
- Gaillardet J., Allègre C.J. (1995) Boron isotopic compositions of corals: Seawater or diagenesis record? *Earth and Planetary Science Letters*, 136: 665-676.
- Giggenbach W.F. (1981) Geothermal mineral equilibria. *Geochimica et Cosmochimica Acta*, 45: 393-410.
- Giggenbach W.F. (1988) Geothermal solute equilibria. Derivation of Na-K-Mg-Ca geothermometers. *Geochim. Cosmochim. Acta*, 52: 2749-2765.
- Giggenbach W.F., Gonfiantini R., Jangi B.L., Truesdell A.H. (1983) Isotopic and chemical compositions of Parbati Valley geothermal discharges, Northwest Himalaya, India. *Geothermics*, 12: 199-222.
- Girard J.P., Guerrot C., Millot R., Casanova J., Blanc P, Gaucher E. (2006) Apport des isotopes du B, Li et Fe à la compréhension des interactions et transferts dans les argilites du Callovo-Oxfordien. Rapport final. BRGM/RP-55216-FR, 122 p.
- Goldstein S.J., Jacobsen S.B. (1987) The Nd and Sr Isotopic systematics of river-water dissolved material: implications for the sources of Nd and Sr in seawater. *Chem. Geol.*, 66: 245-272.
- Gonfiantini R., Tonarini S., Gröning M., Adorni-Braccesi A., Al-Amman A.S., Astner M., Bächler S., Barnes R.M., Bassett R.L., Cocherie A., Deyhle A., Dini A., Ferrara G., Gaillardet J., Grimm J., Guerrot C., Krähenbühl U., Layne G., Lemarchand D., Meixner A., Northington D.J., Pennisi M., Reitznerová E., Rodushkin I., Sugiura N., Surberg R., Tonn S., Wiedenbeck M., Wunderli S., Xiao Y., Zack T. (2003) Intercomparison of boron isotope and concentration measurements. Part II: Evaluation of results. *Geostandards Newsletter*, 27, 1, 41-57.
- Hall J.M. , Chan L.H., McDonough W.F., Turekian K.K. (2005) Determination of the lithium isotopic composition of planktic foraminifera and its application as a paleo-seawater proxy. *Marine Geology*, 217: 255-265.

- Hamon Y. (2001) *Sédimentologie, géométrie et signification géodynamique des dépôts réservoirs silicoclastiques du Trias/Rhétien de Chemery (Sologne, SW du bassin de Paris)*. Mémoire DEA Université Montpellier II.
- Hathorne E.C., James R.H. (2006) Temporal record of lithium in seawater: A tracer for silicate weathering? *Earth and Planetary Science Letters*, 246: 393-406.
- Helgeson H.C., Delany J.M., Nesbitt H.W., Bird D.K. (1978) Summary and critique of the thermodynamic properties of rock-forming minerals. *Amer. Jour. Sci.*, 278A.
- Hoefs J., Sywall M. (1997) Lithium isotope composition of Quaternary biogene carbonates and a global lithium isotope balance. *Geochimica et Cosmochimica Acta*, 61: 2679-2690.
- Hubert A., Bourdon B., Pili E., Meynadier L. (2006) Transport of radionuclides in an unconfined chalk aquifer from U-series disequilibria. *Geochimica et Cosmochimica Acta*, 70: 5437-5454.
- Huh Y., Chan L.C., Zhang L., Edmond J.M. (1998) Lithium and its isotopes in major world rivers: implications for weathering and the oceanic budget. *Geochimica et Cosmochimica Acta*, 62: 2039-2051.
- Huh Y., Chan L.C., Edmond J.M. (2001) Lithium isotopes as a probe of weathering processes: Orinoco River. *Earth and Planetary Science Letters*, 194: 189-199.
- Huh Y., Chan L.C., Chadwick O.A. (2004) Behavior of lithium and its isotopes during weathering of Hawaiian basalt. *Geochemistry, Geophysics, Geosystems*, 5: 1-22.
- Innocent C., Fléhoc C., Lemeille F. (2005) U-Th vs. AMS <sup>14</sup>C dating of shells from the Achenheim loess (Rhine Graben). *Bulletin de la Société Géologique de France*, 176: 249-255.
- Ivanovitch M., Fröhlich K., Hendry M.J. (1991) Uranium-series radionuclides in fluids and solids from the Milk River aquifer, Alberta, Canada. *Applied Geochemistry*, 6: 405-418.
- James R.H., Palmer M.R. (2000) The lithium isotope composition of international rock standards. *Chemical Geology*, 166: 319-326.
- Kharaka Y.K., Lico M.S., Law-Leroy L.M. (1982) Chemical geothermometers applied to formation waters, Gulf of Mexico and California basins. *Am. Assoc. Petrol. Geol. Bull.*, 66: 588.
- Kharaka Y.K., Specht B.J., Carothers W.W. (1985) Low-to-intermediate subsurface temperatures calculated by chemical geothermometers. *The American Association of Petroleum Geologists. Annual Convention, Book of Abstracts, New Orleans*, 24-27.

- Kharaka Y.K., Mariner R.H. (1989) Chemical geothermometers and their application to formation waters from sedimentary basins. In: Naeser, N.D. and McCulloch, T.H. (eds), Thermal history of sedimentary basins: methods and case histories. Springer-Verlag, New York: 99-117.
- Kisakürek B., Widdowson M., James R.H. (2004) Behaviour of Li isotopes during continental weathering: the Bidar laterite profile, India. *Chemical Geology*, 212: 27-44.
- Kisakürek B., James R.H., Harris N.B.W. (2005) Li and  $\delta^7\text{Li}$  in Himalayan rivers: Proxies for silicate weathering? *Earth and Planetary Science Letters*, 237: 387-401.
- Koepnick R.B., Denison R.E., Burke W.H., Hetherington E.A., Dahl D.A. (1990) Construction of the Triassic and Jurassic portion of the Phanerozoic curve of seawater  $^{87}\text{Sr}/^{86}\text{Sr}$ . *Chem. Geol.*, 80: 327-349.
- Lemarchand E., Chabaux F., Vigier N., Millot R., Pierret M.C. (2010) Lithium isotope systematics in a forested granitic catchment (Strengbach, Vosges Mountains, France). *Geochimica et Cosmochimica Acta*, 74: 4612-4628.
- Maget Ph. (1983) Potentiel géothermique "basse température" en France. Rapport BRGM 83, SGN 375 SPG Ed.
- Matray J.M., Meunier A., Thomas M., Fontes J.Ch. (1989) Les eaux de formation du Trias et du Dogger du bassin parisien : histoire et effets diagénétiques sur les réservoirs. *Soc. Nat Elf-Aquitaine*, 483-504.
- Matray J.M., Lambert M., Fontes J.Ch. (1994) Stable isotope conservation and origin of saline waters from the Middle Jurassic aquifer of the Paris Basin, France. *Applied Geochemistry*, 9: 297-309.
- Marty B., Dewonck S., France-Lanord C. (2003) Geochemical evidence for efficient aquifer isolation over geological timeframes. *Nature*, 425: 55-58.
- Michard G. (1979) Géothermomètres chimiques. *Bull. BRGM (2) III*, n°2: 183-189.
- Michard G. (1990) Behaviour of major elements and some trace elements (Li, Rb, Cs, Sr, Fe, Mn, W, F) in deep hot waters from granitic areas. *Chem. Geol.*, 89: 117-134.
- Millot R., Guerrot C., Vigier N. (2004) Accurate and high precision measurement of lithium isotopes in two reference materials by MC-ICP-MS. *Geostandards and Geoanalytical Research*, 28: 53-159.
- Millot R., Négrel Ph., Petelet-Giraud E. (2007) Multi-isotopic (Li, B, Sr, Nd) approach for geothermal reservoir characterization in the Limagne Basin (Massif Central, France) *Applied Geochemistry*, 22: 2307-2325.

- Millot R., Négrel Ph. (2007) Multi-isotopic tracing ( $\delta^7\text{Li}$ ,  $\delta^{11}\text{B}$ ,  $^{87}\text{Sr}/^{86}\text{Sr}$ ) and chemical geothermometry: evidence from hydro-geothermal systems in France. *Chemical Geology*, 244: 664-678.
- Millot R., Petelet-Giraud E., Guerrot C., Négrel Ph. (2010a) Multi-isotopic composition ( $\delta^7\text{Li}$ - $\delta^{11}\text{B}$ - $\delta\text{D}$ - $\delta^{18}\text{O}$ ) of rainwaters in France: origin and spatio-temporal characterization *Applied Geochemistry*, 25: 1510-1524.
- Millot R., Vigier N., Gaillardet J. (2010b) Behaviour of lithium and its isotopes during weathering in the Mackenzie Basin, Canada. *Geochimica et Cosmochimica Acta*, 74: 3897-3912.
- Millot R., Scaillet B., Sanjuan B. (2010c) Lithium isotopes in island arc geothermal systems: Guadeloupe, Martinique (French West Indies) and experimental approach. *Geochimica et Cosmochimica Acta*, 74: 1852-1871.
- Mossadik H. (1997) Les isotopes du bore, traceurs naturels dans les eaux. Mise au point de l'analyse en spectrométrie de masse à source solide et application à différents environnements. PhD Thesis, Université d'Orléans, Orléans.
- Négrel Ph., Fouillac C. Brach M. (1997) Occurrence of mineral water springs in the stream channel of the Allier River (Massif Central, France): chemical and Sr isotope constraints. *J. of Hydrol.*, 203: 143-153.
- Négrel Ph. (1999) Geochemical study in a granitic area, the Margeride, France: chemical element behavior and  $^{87}\text{Sr}/^{86}\text{Sr}$  constraints. *Aquatic Geochemistry*, 5: 125-165.
- Négrel Ph., Guerrot C., Cocherie A., Azaroual M., Brach M., Fouillac C. (2000) Rare Earth Elements, neodymium and strontium isotopic systematics in mineral waters: evidence from the Massif Central, France. *Applied Geochemistry*, 15: 1345-1367.
- Négrel Ph., Guerrot C., Millot R. (2007) Chemical and strontium isotope characterization of rainwater in France: influence of sources and hydrogeochemical implications. *Isotopes in Environmental and Health Studies*, 43: 179-196.
- Nicholson K. (1993) *Geothermal fluids. Chemistry and Exploration Techniques*. Springer, 261 p.
- Pin C., Bassin C. (1992) Evaluation of a strontium specific extraction chromatographic method for isotopic analysis in geological materials. *Anal. Chim. Acta*, 269: 249-255.
- Pinti D.L., Marty B. (1995) Noble gases in crude oils from the Paris Basin, France: Implications for the origin of fluids and constraints on oil-water-gas interactions. *Geochimica et Cosmochimica Acta*, 59: 3389-3404.
- Pogge von Strandmann P.A.E., Burton K.W., James R.H., van Calsteren P., Gislason S.R., Mokadem F. (2006) Riverine behaviour of uranium and lithium isotopes in an actively glaciated basaltic terrain. *Earth and Planetary Science Letters*, 251: 134-147.

- Pomerol C. (1974) Le bassin de Paris. In: *Geologie de la France* (ed. by J. Debelmas). 230-258, Doin, Paris.
- Pistiner J.S., Henderson G.M. (2003) Lithium isotope fractionation during continental weathering processes. *Earth and Planetary Science Letters*, 214: 327-339.
- Rosenberg P.E., Kittrick J.A. (1990) Muscovite dissolution at 25°C: Implications for Illite/Smectite-Kaolinite stability relations. *Clay and Clay Minerals*, 38: 445-447.
- Rittenhouse G. (1967) Bromine in oil-field waters and its use in determining possibilities of origin of these waters. *Amer. Ass. of Petroleum Geol. Bull.*, 51: 2430-2440.
- Sanjuan B., Girard J.-P., Lanini S., Bourguignon A., Brosse E. (2003) Geochemical modelling of diagenetic illite and quartz cement formation in Brent sandstone reservoirs: Example of the Hild field, Norwegian North Sea. In: *Clay Mineral Cements in Sandstones* edited by R.H. Worden and S. Morad, Blackwell Publishing, Int. Assoc. Sedimentol. Spec. Publ. 34: 425-452.
- Serra H., Sanjuan B. (2004) Synthèse bibliographique des géothermomètres chimiques. Report BRGM/RP-52430-FR, 80 p.
- Spivack A.J., Edmond J.M. (1986) Determination of boron isotope ratios by thermal ionisation mass spectrometry of the dicesium metaborate cation. *Analytical Chemistry*, 58: 31-35.
- Spivack A.J., Edmond J.M. (1987) Boron isotope exchange between seawater and the oceanic crust. *Geochimica et Cosmochimica Acta*, 51: 1033-1043.
- Teng F.Z., McDonough W.F., Rudnick R.L., Dalpé C., Tomascak P.B., Chappell B.W., Gao S. (2004) Lithium isotopic composition and concentration of the upper continental crust. *Geochimica et Cosmochimica Acta*, 68: 4167-4178.
- Tomascak P.B. (2004) Developments in the Understanding and Application of Lithium Isotopes in the Earth and Planetary Sciences. In *Reviews in Mineralogy & Geochemistry*, 55: 153-195.
- Truesdell A.H. (1976) Geochemical techniques in exploration, summary of section III. *Proc. Sec. United Nations Symp. Develop. Use Geotherm. Res.*, San Francisco, 53-79.
- Vigier N., Rollion-Bard C., Spezzaferri S., Brunet F. (2007) In-situ measurements of Li isotopes in foraminifera. *Geochemistry, Geophysics, Geosystems* Q01003.

- Vigier N., Gislason S.R., Burton K.W., Millot R., Mokadem F. (2009) The relationship between riverine lithium isotope composition and silicate weathering rates in Iceland. *Earth and Planetary Science Letters*, 287: 434-441.
- Wasserburg G.J., Jacobsen S.B., De Paolo D.J., McCulloch M.T., Wen T. (1981) Precise determination of Sm/Nd ratios, samarium, and neodymium isotopic abundances in standard solutions. *Geochimica et Cosmochimica Acta*, 45:2311-2323.
- Weissberg B.G., Wilson P.T. (1977) Montmorillonite and the Na/K geothermometer. In *Geochemistry 77*, N.Z. Dept. Sci. Indust. Res. Bull., 218: 31-35.
- White D.E. (1965) Saline waters of sedimentary rocks. *Fluids in Subsurface Environments - A Symposium*. Am. Ass. Petrol. Geol. Mem., 4: 342-366.
- White D.E. (1970) Geochemistry applied to the discovery, evaluation, and exploitation of geothermal energy resources, *Geothermics, Special Issue 2 on U.N. Symposium on the development and utilization of geothermal resources, Pisa, Italy, vol. 1, section V*, 58-80.
- Williams L.B., Hervig R.L., Holloway J.R., Hutcheon I. (2001a) Boron isotope geochemistry during diagenesis. Part II. Experimental determination of fractionation during illitization of smectite. *Geochimica et Cosmochimica Acta*, 65: 1769-1782.
- Williams L.B., Hervig R.L., Hutcheon I. (2001b) Boron isotope geochemistry during diagenesis Part II. Application to organic-rich sediments. *Geochimica et Cosmochimica Acta*, 65: 1783-1794.
- Wolery T.J. (1995) EQ3NR. A computer program for geochemical aqueous speciation-solubility calculations. Theoretical manual, user's guide, and related documentation (version 7.0), 246 p.
- Worden R.H., Coleman M.L., Matray J.M. (1999) Basin scale evolution of formation waters: A diagenetic and formation water study of the Triassic Chaunoy Formation, Paris Basin. *Geochimica et Cosmochimica Acta*, 63: 2513-2528.

## Table captions

### Table 1

Physicochemical measurements of water samples: sampling temperature, pH, Eh (mV), conductivity (mS/cm) and alkalinity (meq/L).

### Table 2

Major cations and anions (Na, K, Mg, Ca, Cl, Br, SO<sub>4</sub>, SiO<sub>2</sub> mg/L), Li, B, Sr (mg/L), U concentrations (ng/L), Cl/Br ratios and Total Dissolved Solids (TDS, in g/L) for Triassic formation waters of the Paris Basin.

### Table 3

Stable isotopes of the water molecule ( $\delta D$  and  $\delta^{18}O$ , ‰), Sr isotopic ratios ( $^{87}Sr/^{86}Sr$ ), Li isotopic ratios ( $\delta^7Li$ , ‰), B isotopic ratios ( $\delta^{11}B$ , ‰) and  $^{234}U/^{238}U$  activity ratios for Triassic formation waters of the Paris Basin.

### Table 4

Estimates of deep underground temperatures by chemical geothermometry for Triassic formation waters of the Paris Basin.

### Table 5

Saturation indices (SI) in two representative samples of Triassic formation waters for the principal mineral phases (under reservoir temperature conditions) determined using the geochemical code EQ3NR (Wolery 1995). The Chaunoy72 water sample is representative of waters from the central part of the Paris Basin (Chaunoy73 and Champotran samples having almost the same chemical composition). The Châteauroux water sample is representative of the recharge area.

## Figure captions

### Figure 1

Schematic cross-section of deep aquifers formations in the Paris Basin (from Maget 1983) and location of the five sampling sites (Chaunoy, Champotran, La Torche, Châteauroux and Santenay).

### Figure 2

Cl concentrations (mg/L) plotted as a function of Na concentrations (mg/L) for Chaunoy, Champotran, La Torche, Châteauroux and Santenay samples. Seawater value, seawater dilution line and data from the literature are also shown.

### Figure 3

Cl/Br ratio vs. Cl concentration. This graph was modified from Matray et al. (1989). The Châteauroux water sample (GTH01) is not shown on this graph because the Br content is lower than the limit of quantification for this sample (0.1 mg/L). However, we know that Cl = 12.7 mg/L and, therefore,  $\text{Log}(\text{Cl}) = 1.1$  and  $\text{Log}(\text{Cl}/\text{Br}) > 2.1$ . The X-axis represents the dilution effect, whereas the Y-axis is the saumure type.

### Figure 4

$\delta\text{D}$  vs.  $\delta^{18}\text{O}$  values for Triassic formation waters (Figure 4a). Data from the literature are from Fontes and Matray (1993a, 1993b) and Marty et al. (2003). The Global Meteoric Water Line (GMWL) has also been drawn, for comparison,  $\delta\text{D} = 8 \times \delta^{18}\text{O} + 10$  (Craig 1961).  $\delta\text{D}$  and  $\delta^{18}\text{O}$  values vs. Cl concentrations (mg/L) for Triassic formation waters (Figure 4b and 4c).  $\delta^{18}\text{O}$  values in water samples according to the estimated distance from the recharge zone (Figure 4d). An error of 10% was assigned to this estimate. A distance of 0 km was used for the Santenay location.

### Figure 5

Sr isotopic ratios ( $^{87}\text{Sr}/^{86}\text{Sr}$ ) plotted as a function of Sr concentration (mg/L) for Triassic formation waters in the Paris Basin. Data from the literature are from Fontes and Matray (1993a, 1993b).

### Figure 6

Li isotopic ratios ( $\delta^7\text{Li}$ , ‰) plotted as a function of Li concentration (mg/L) for Triassic formation waters in the Paris Basin. Data for the Dogger formation are from Girard et al. (2006).

#### **Figure 7**

B isotopic ratios ( $\delta^{11}\text{B}$ , ‰) plotted as a function of B concentration (mg/L) for Triassic formation waters in the Paris Basin. Data for the Dogger formation are from Girard et al. (2006).

#### **Figure 8**

Uranium ( $^{234}\text{U}/^{238}\text{U}$ ) activity ratios plotted as a function of U concentration (Log scale, ng/L) for Triassic formation waters in the Paris Basin. The field for Dogger formation waters is from Casanova et al. (2006), and for the Upper Cretaceous chalk aquifer from Hubert et al. (2006).

#### **Figure 9**

Multi-isotope characterization of Triassic formation waters in the Paris Basin: B isotopes vs. Sr isotopes (Figure 9a), Li isotopes vs. Sr isotopes (Figure 9b) and B isotopes vs. Li isotopes (Figure 9c). Continental rocks have  $\delta^7\text{Li}$  values ranging from -2 to +2‰ (Teng et al. 2004 and reference therein), whereas most carbonates analysed so far have  $\delta^7\text{Li}$  values between +6 and > 25‰ (e.g. Hoefs and Sywall 1997, Hall et al. 2005, Hathorne and James 2006, Vigier et al. 2007). B isotopic compositions for the principal crustal lithologies are well constrained with  $\delta^{11}\text{B}$  values ranging from -10 to 0‰, and from +15 to +30‰, for granite and gneiss and carbonate, respectively (Barth 1993, 2000). The field for Li and B isotopes in rainwaters is from Millot et al. (2010a), and from Négrel et al. (2007) for Sr isotopes.

#### **Figure 10**

Evolution of the uranium ( $^{234}\text{U}/^{238}\text{U}$ ) activity ratio in water samples depending on the estimated distance from the recharge zone. An error of 10% was assigned to this estimate. A distance of 0 km was used for the Santenay location. We did perform two different calculations to test the efficiency of our approach. For curve #1, all the data points are considered. For curve #2, we did the same calculation without the samples from Santenay. See text for comments.

Table 1

location	sample name	sampling date	sampling temperature °C	depth m	water content %	pH	Eh mV	Cond. 25°C mS/cm	Alk. meq/L
CHAUNOY	Chaunoy 72	26/11/2007	83	2734	97	6.30	-150	-	1.28
	Chaunoy 73	27/11/2007	43	2449	97	6.00	-490	-	1.23
LA TORCHE	LT09	27/11/2007	29	2923	49	4.44	-	-	0.22
CHAMPOTRAN	CHAN25	27/11/2007	35	2989	15.6	6.50	-	-	2.22
CHATEAUROUX	GTH01	04/04/2008	33.2*	623	100	7.80	-120	0.32	4.85
SANTENAY	Lithium	06/05/2008	18.1*	75	100	6.95	-8	13.46	8.98
	Santana	06/05/2008	17.8*	88	100	7.01	-10	13.39	7.77

\*: temperature at the surface

Table 2

location	sample name	Na mg/L	K mg/L	Mg mg/L	Ca mg/L	Cl mg/L	SO <sub>4</sub> mg/L	Br mg/l	SiO <sub>2</sub> mg/L	Cl/Br	TDS g/L	B mg/L	Li mg/L	Sr mg/L	U ng/L
CHAUNOY	Chaunoy 72	37300	966	1127	7055	77000	659	704	47.0	109.4	125	51	42	350	6.6
	Chaunoy 73	36700	972	1068	5841	73500	704	673	49.6	109.2	120	52	40	300	3.6
LA TORCHE	LT09	52000	1954	1183	8339	102000	462	990	33.1	103.0	168	120	48	495	6.1
CHAMPOTRAN	CHAN25	36200	952	1010	5600	72000	685	633	40.3	113.7	118	58	36.3	287	83.0
CHATEAUROUX	GTH01	55.1	7.9	8.8	20.1	12.7	26.6	< 0.1	15.2	-	0.37	0.32	0.23	0.85	49.2
SANTENAY	Lithium	2820	112	26.3	349	3500	2352	18.3	18.1	191.3	9.52	5.30	19.70	10.34	3654
	Santana	2803	112	24.6	328	3400	2479	15.6	17.2	217.9	9.52	5.36	19.37	9.80	4525

Table 3

location	sample name	$\delta D$ (‰) +/- 0.8‰	$\delta^{18}O$ (‰) +/- 0.1‰	$^{87}Sr/^{86}Sr$	2 $\sigma$	$\delta^{7}Li$ (‰) 2 $\sigma_m$	$\delta^{11}B$ (‰) 2 $\sigma_m$	$^{234}U/^{238}U$	2 $\sigma$		
<b>CHAUNOY</b>	Chaunoy 72	-20.9	-2.7	0.711232	0.000009	7.1	0.2	25.3	0.1	1.365	0.011
	Chaunoy 73	-19.6	-2.5	0.710976	0.000009	6.8	0.2	25.5	0.1	1.935	0.027
<b>LA TORCHE</b>	LT09	-7.6	-0.9	0.710432	0.000007	10.9	0.1	22.5	0.1	1.138	0.020
<b>CHAMPOTRAN</b>	CHAN25	-20.7	-2.5	0.710971	0.000008	6.7	0.1	25.4	0.2	1.187	0.003
<b>CHATEAUROUX</b>	GTH01	-52.2	-7.9	0.710468	0.000007	9.3	0.2	17.0	0.1	6.064	0.019
<b>SANTENAY</b>	Lithium	-55.6	-8.3	0.715855	0.000010	7.2	0.1	5.9	0.1	8.912	0.028
	Santana	-55.5	-8.3	0.715974	0.000008	7.3	0.1	5.1	0.1	9.637	0.021

Table 4

location	sample name	depth m	sampling temperature °C	T <sub>calculated</sub> °C	T <sub>SiO2-Oz</sub> °C	T <sub>Chalced. (1)</sub> °C	T <sub>Chalced. (2)</sub> °C	T <sub>Na/K (1)</sub> °C	T <sub>Na/K (2)</sub> °C	T <sub>Na/K/Ca (β=1/3)</sub> °C	T <sub>Na/K/Ca/Mg</sub> °C	T <sub>K/Mg</sub> °C	T <sub>Na/Li (1)</sub> °C	T <sub>Na/Li (2)</sub> °C	T <sub>Mg/Li</sub> °C
CHAUNOY	Chaunoy 72	2734	83	95 ± 20	99	69	77	123	88	153	85	125	153	83	136
	Chaunoy 73	2449	43	95 ± 20	102	72	79	124	89	156	78	126	152	81	136
LA TORCHE	L.T09	2923	29	85 ± 20	84	54	62	145	112	176	99	147	144	72	140
CHAMPOTRAN	CHAN25	2989	35	90 ± 20	92	62	70	124	88	155	79	126	148	77	133
CHATEAUROUX	GTH01	623	33.2*	45 ± 10	54	24	33	249	239	180	37	62	231	174	61
SANTENAY	Lithium	75	18.1*	50 ± 10	60	30	40	148	116	157	129	116	269	223	177
	Santana	88	17.8*	50 ± 10	58	28	38	149	117	157	130	117	268	222	178

\*: temperature at the surface

T<sub>SiO2-Oz</sub>: Fournier and Rowe (1966), T<sub>Chalced. (1)</sub>: Arnorsson et al. (1983), T<sub>Chalced. (2)</sub>: Helgeson et al. (1978)

T<sub>Na/K (1)</sub>: Fournier (1979), T<sub>Na/K (2)</sub>: Michard (1979)

T<sub>Na/K/Ca</sub>: Fournier and Truesdell (1973), T<sub>Na/K/Ca/Mg</sub>: correction with Mg (Fournier and Potter 1979)

T<sub>K/Mg</sub>: Giggenbach (1988)

T<sub>Na/Li (1)</sub>: Kharaka et al. (1982), T<sub>Na/Li (2)</sub>: Fouillac et Michard (1981)

T<sub>Mg/Li</sub>: Kharaka and Mariner (1989)

**Table 5**

<b>Saturation Index</b>	<b>Chaunoy 72</b>	<b>Châteauroux GTH01</b>
Albite	-0.26	-2.21
Anhydrite	-0.02	-2.68
Aragonite	-0.14	0.14
Barytine	0.04	0.22
Calcite	0.00	0.28
Celestite	-0.89	-3.14
Chalcedony	-0.24	-0.20
Dolomite	0.90	1.69
K-Feldspar	0.00	-0.55
Kaolinite	-0.88	-1.14
Magnesite	-0.37	-0.10
Na-Montmorillonite	0.01	-0.80
K-Montmorillonite	-0.39	-0.87
Ca-Montmorillonite	0.02	-0.43
Mg-Montmorillonite	0.12	-0.32
Muscovite	0.26	-0.84
Quartz	-0.03	0.06
Siderite	-0.95	-0.85
Strontianite	-0.31	0.54

Figure 1

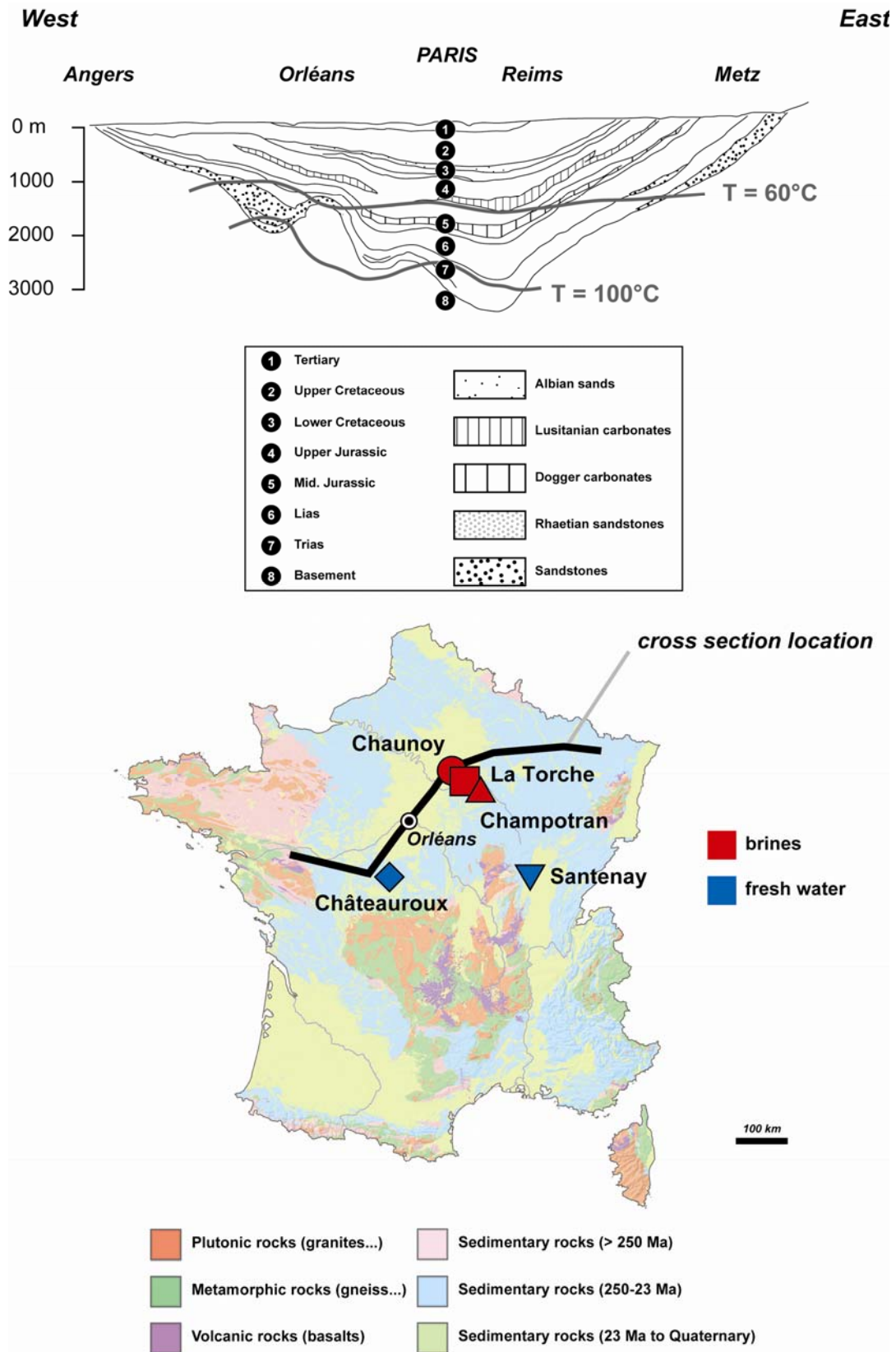


Figure 2

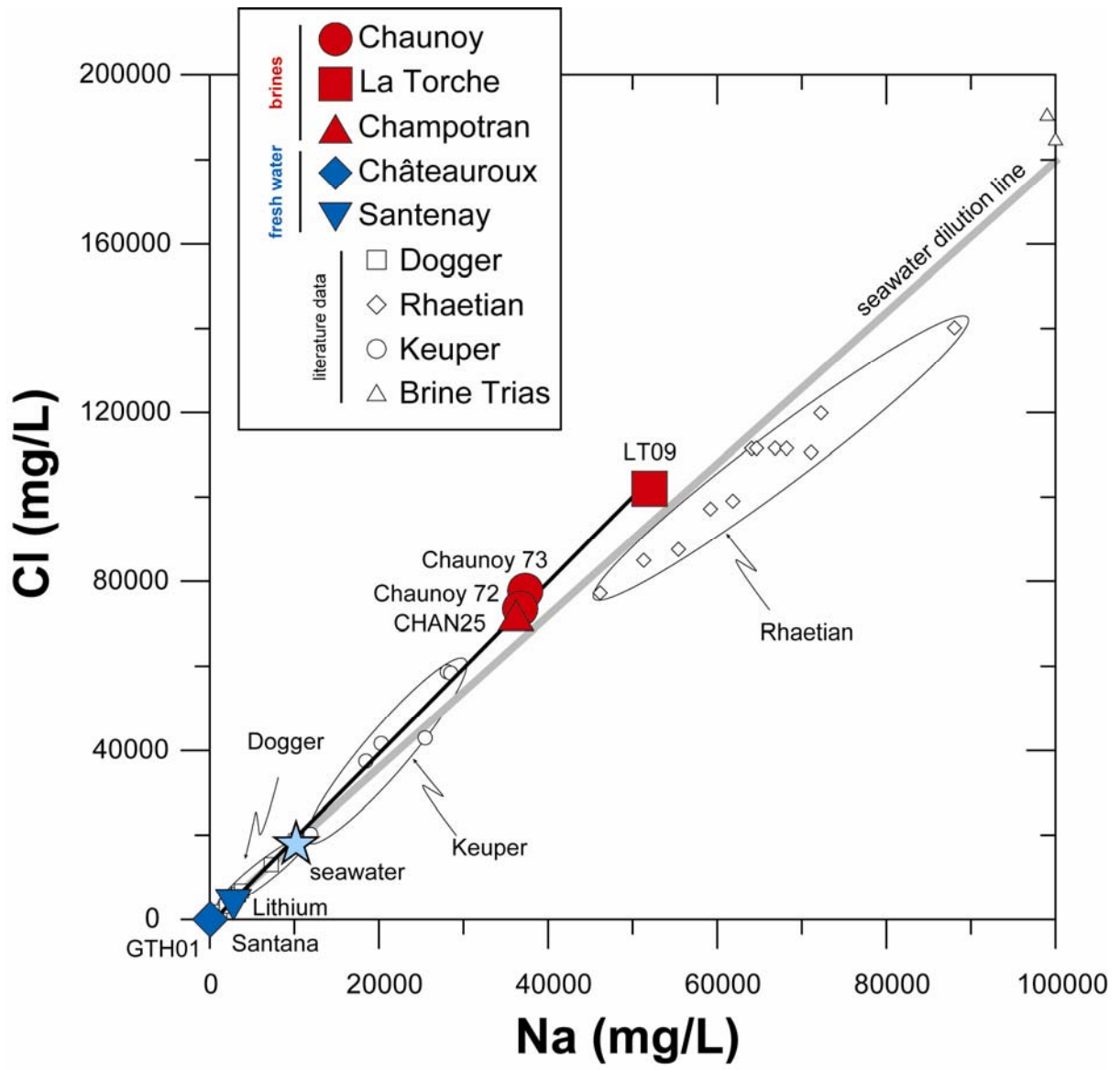


Figure 3

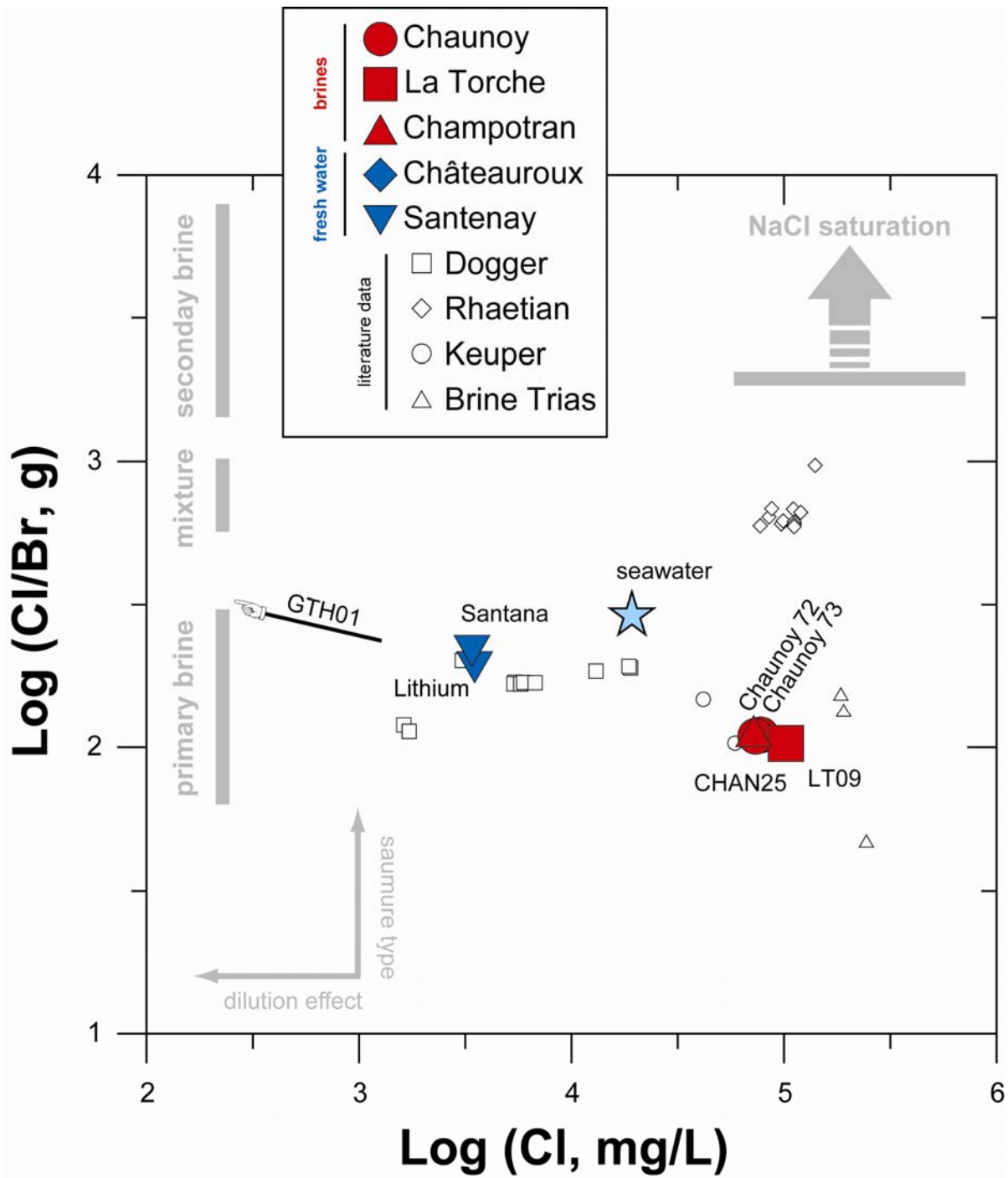


Figure 4

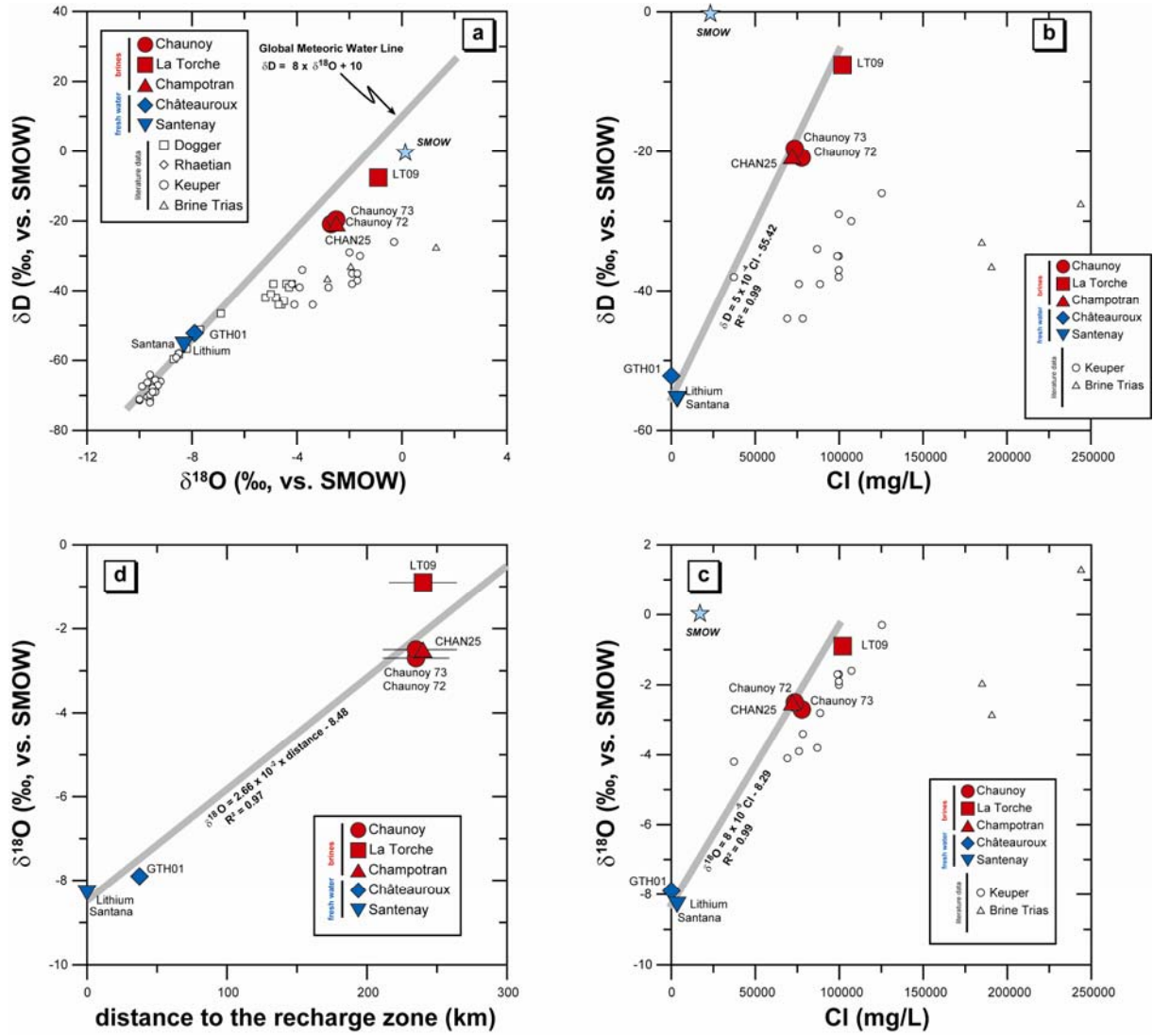


Figure 5

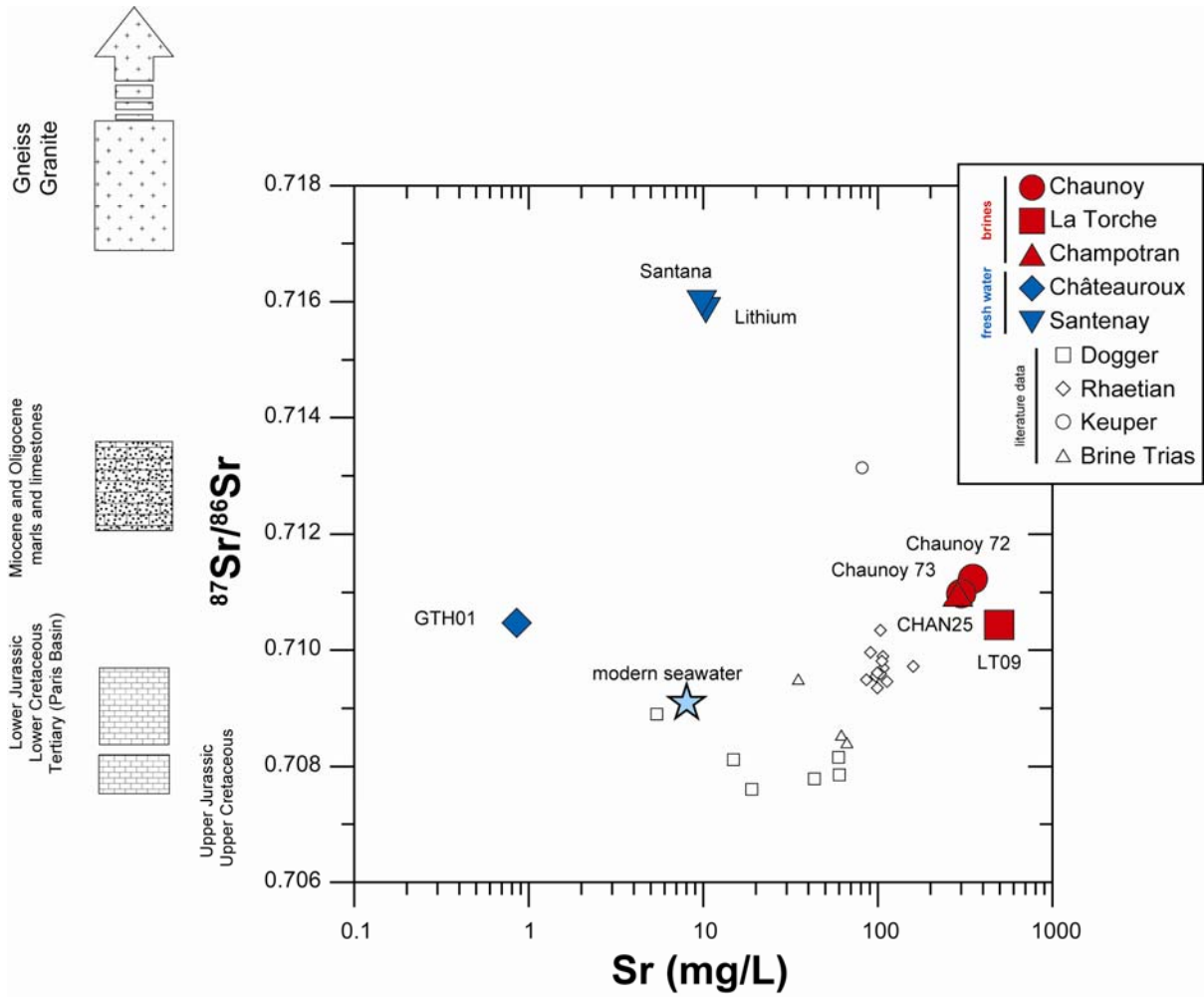


Figure 6

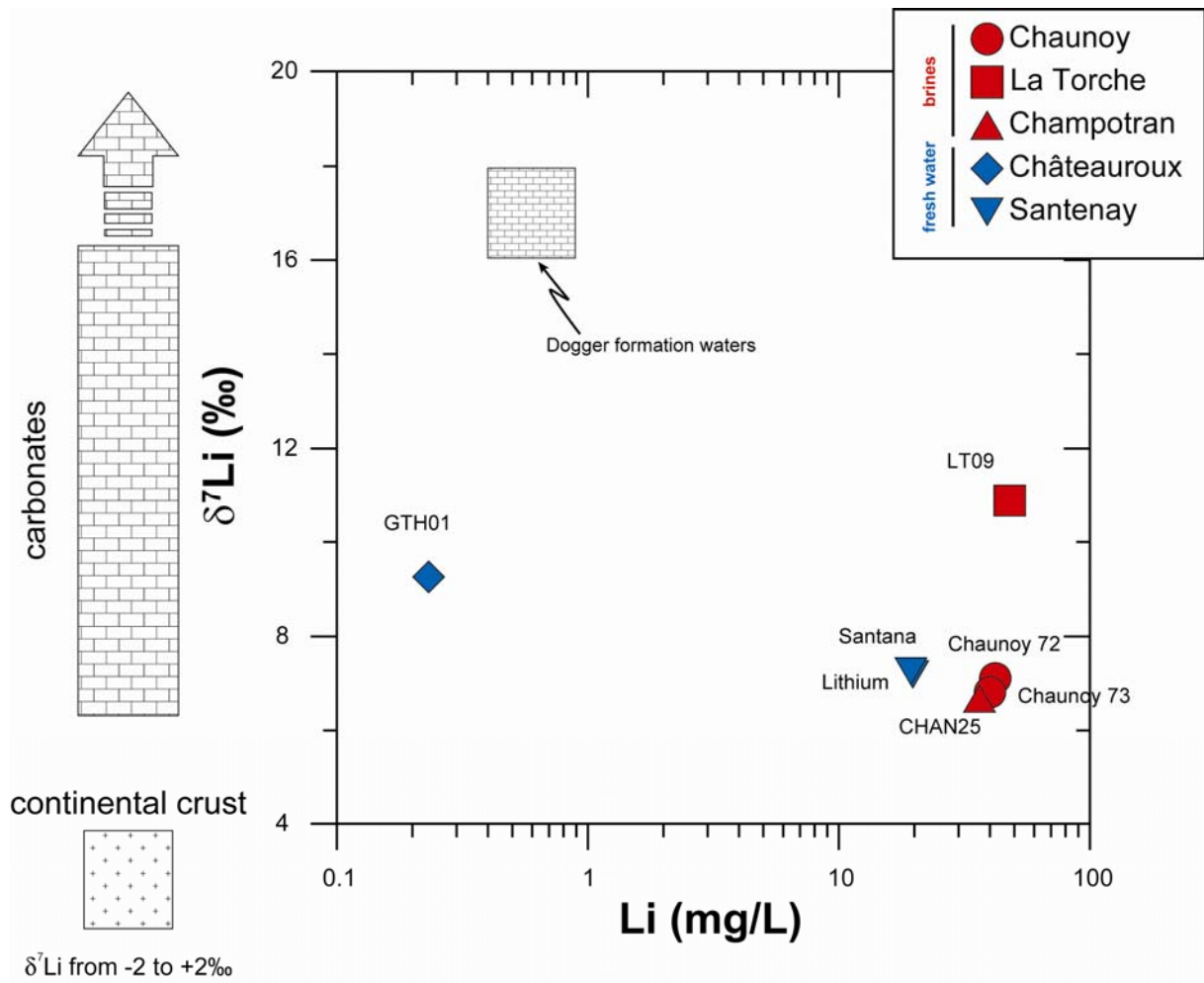


Figure 7

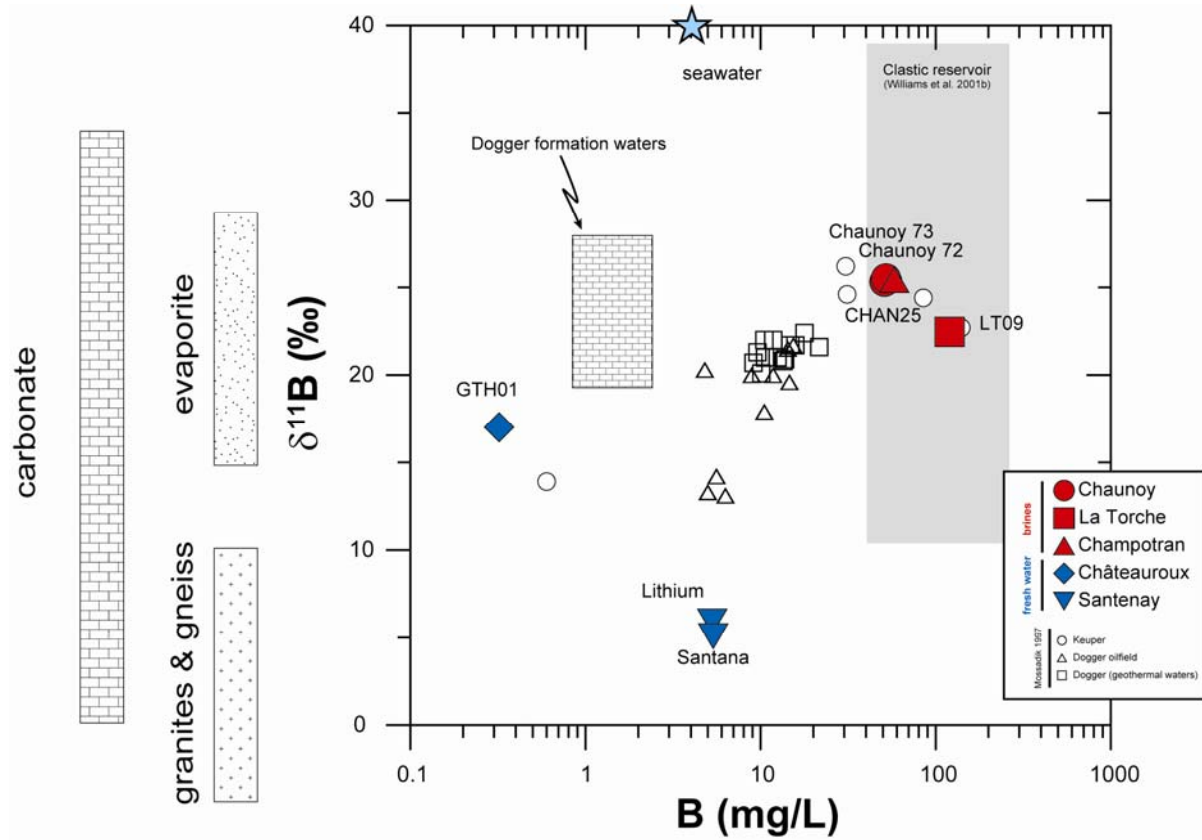


Figure 8

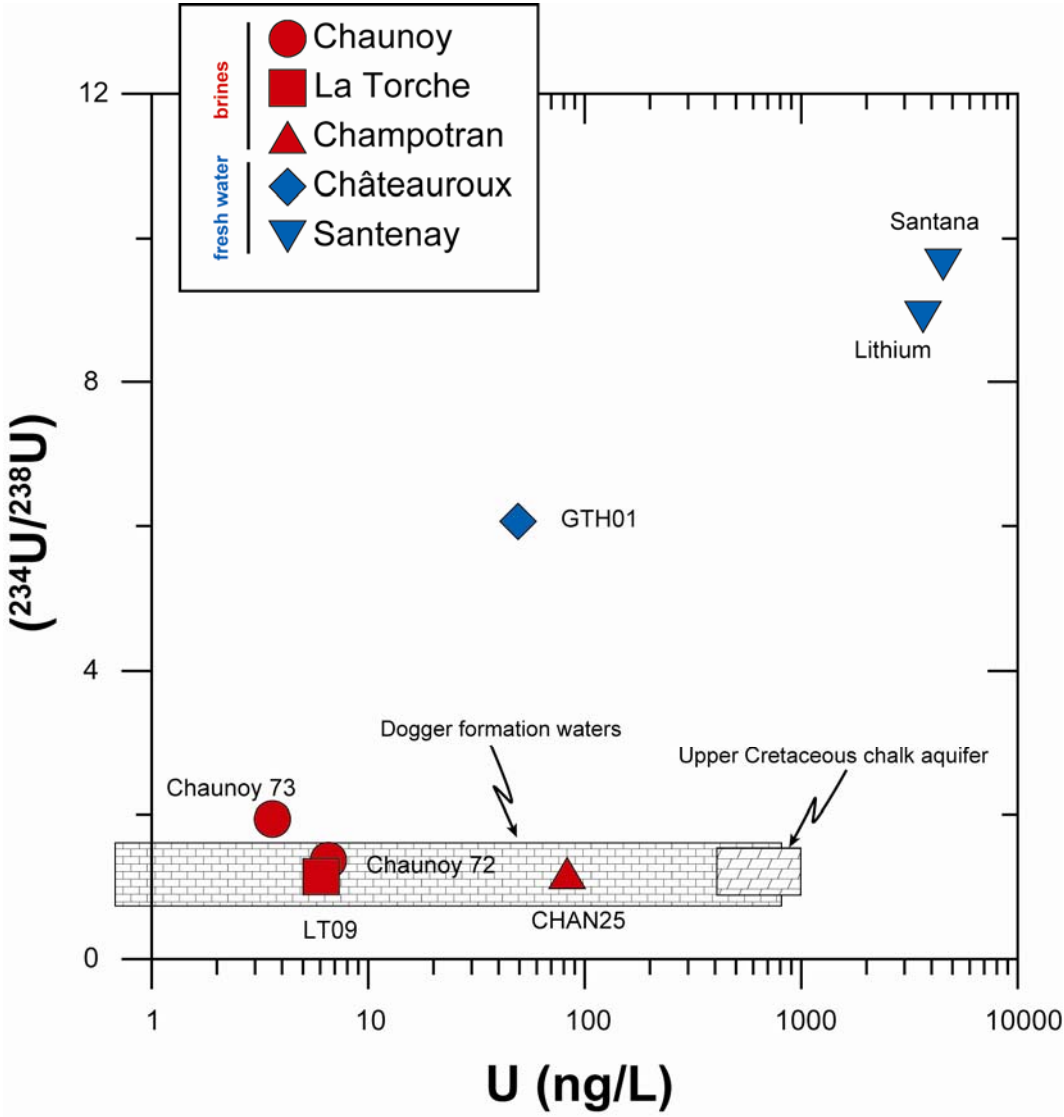


Figure 9

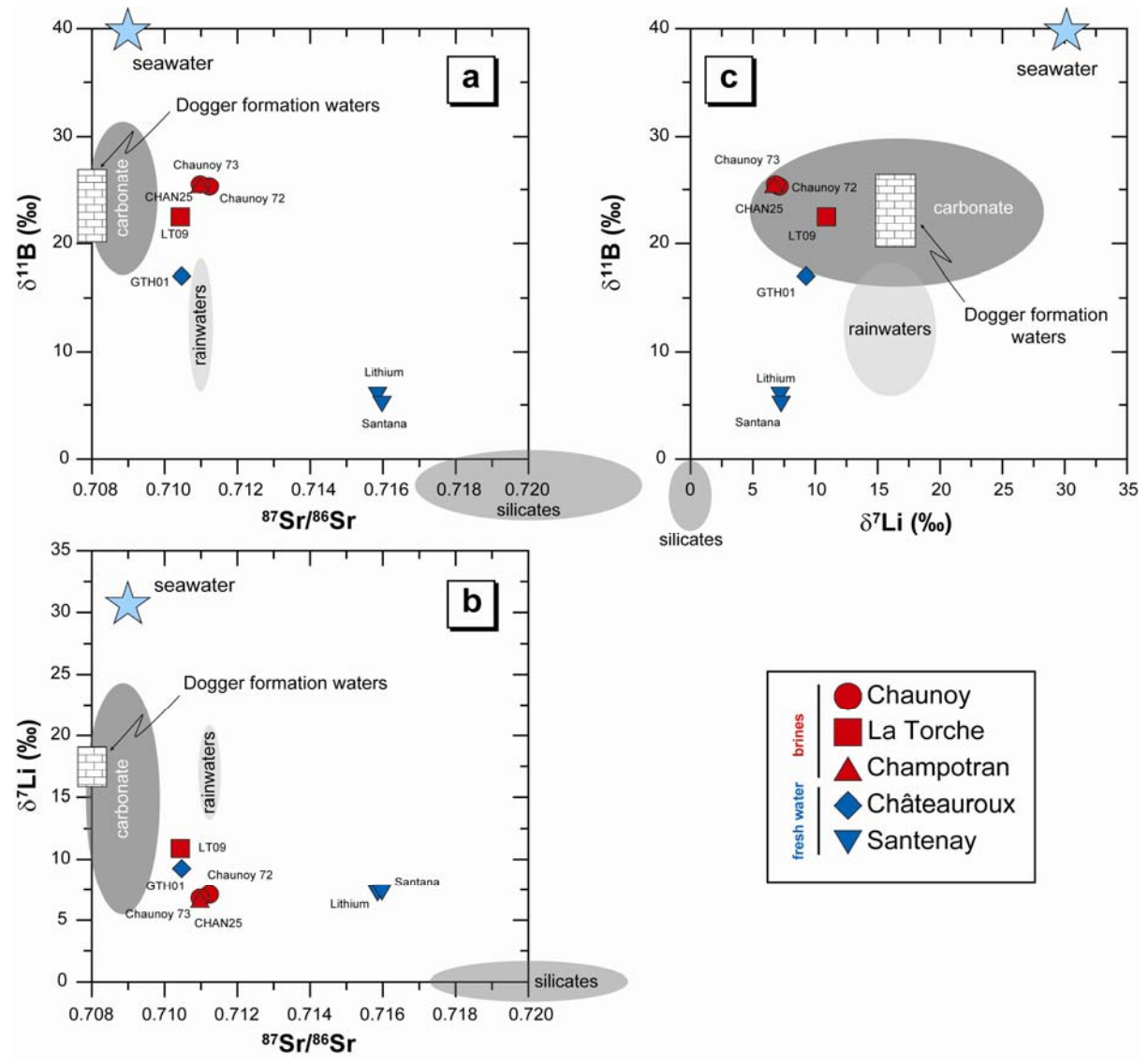


Figure 10

